

On natural frequencies of Levy-type thick porous-cellular plates surrounded by piezoelectric layers

Original

On natural frequencies of Levy-type thick porous-cellular plates surrounded by piezoelectric layers / Askari, M., Saidi, A.R., Rezaei, A.S.. - In: COMPOSITE STRUCTURES. - ISSN 0263-8223. - 179:(2017), pp. 340-354.
[10.1016/j.compstruct.2017.07.073]

Availability:

This version is available at: 11583/2840764 since: 2020-07-27T12:19:28Z

Publisher:

Elsevier Ltd

Published

DOI:10.1016/j.compstruct.2017.07.073

Terms of use:

This article is made available under terms and conditions as specified in the corresponding bibliographic description in the repository

Publisher copyright

Elsevier postprint/Author's Accepted Manuscript

© 2017. This manuscript version is made available under the CC-BY-NC-ND 4.0 license
<http://creativecommons.org/licenses/by-nc-nd/4.0/>. The final authenticated version is available online at:
<http://dx.doi.org/10.1016/j.compstruct.2017.07.073>

(Article begins on next page)

Accepted Manuscript

On natural frequencies of Levy-type thick porous-cellular plates surrounded by piezoelectric layers

M. Askari, A.R. Saidi, A.S. Rezaei

PII: S0263-8223(16)32333-9

DOI: <http://dx.doi.org/10.1016/j.compstruct.2017.07.073>

Reference: COST 8728

To appear in: *Composite Structures*

Received Date: 29 October 2016

Revised Date: 19 June 2017

Accepted Date: 19 July 2017



Please cite this article as: Askari, M., Saidi, A.R., Rezaei, A.S., On natural frequencies of Levy-type thick porous-cellular plates surrounded by piezoelectric layers, *Composite Structures* (2017), doi: <http://dx.doi.org/10.1016/j.compstruct.2017.07.073>

This is a PDF file of an unedited manuscript that has been accepted for publication. As a service to our customers we are providing this early version of the manuscript. The manuscript will undergo copyediting, typesetting, and review of the resulting proof before it is published in its final form. Please note that during the production process errors may be discovered which could affect the content, and all legal disclaimers that apply to the journal pertain.

On natural frequencies of Levy-type thick porous-cellular plates surrounded by piezoelectric layers

M. Askari, A. R. Saidi*, A. S. Rezaei

Department of Mechanical Engineering, Shahid Bahonar University of Kerman, Kerman, Iran

Abstract

In this paper, an analytical solution for free vibration of rectangular porous-cellular plates enclosed by piezoelectric layers is presented by using third-order shear deformation plate theory. Using Hamilton's principle and Maxwell equation, the governing equations of the system are obtained for both closed and open circuit conditions. Due to the coordinate dependency of mechanical properties of porous materials, the governing equations of motion are highly coupled. By using four auxiliary functions, these equations convert into two independent partial differential equations. The decoupled equations are solved analytically by employing Levy-type boundary conditions for the plate. Finally, after validation of the obtained results, the effects of various parameters such as porosity and geometrical dimensions on the natural frequencies of plate are investigated for different electrical and mechanical boundary conditions. It is found that the natural frequencies of the plate decrease as the coefficient of plate porosity increases. Also, the piezoelectric layers cause the natural frequency of the plate to increase in various vibrating modes.

Keywords: Free vibration, Levy-type solution, Porous materials, Piezoelectric materials, Third-order shear deformation theory

1. Introduction

In order to analyze the mechanical behavior of plates, several theories are proposed in which the extension of the displacement field along the plate thickness is different and the number of extended terms is directly related to thickness-length ratio of the plate. To analyze the mechanical behavior of thin plates, it is reasonable to use classical plate theory (CPT). In 1951, Mindlin [1] introduced first-order shear deformation theory (FSDT) that can be considered as a modified model of classical theory for moderately thick plates. This theory, due to considering the displacement induced by shear forces, may be considered as a good alternative for classical theory so as to analyze the moderately thick plates. By increasing the number of extended terms, other theories may be obtained. Following this approach, a new higher-order theory; i.e., Reddy's third-order shear deformation theory (TSDT) has been proposed [2].

* Corresponding author. Tel.: +98-34-32111763, fax: +98-34-32120964
E-mail address: saidi@uk.ac.ir (A.R. Saidi)

In general, porous materials due to their unique properties such as high stiffness in conjunction with low specific weight, are widely used in several applications including lightweight structures, energy absorption, sound attenuation and thermal insulation [3].

To analyze the dynamic behavior of rectangular plates, lots of investigations have been performed. Among all notable works, the free vibration analysis of isotropic rectangular plates under different boundary conditions have been carried out by Leissa [4] using CPT. Reddy and Phan [5] presented an exact solution for vibration and stability of isotropic, orthotropic and laminated rectangular plates having simply supported boundary condition on all edges according to a higher-order shear deformation theory. Liew et al. [6] investigated the three-dimensional vibrations of thick rectangular plates made of homogeneous materials with general boundary conditions by using Ritz method. Vel and Batra [7] provided an exact solution for free vibration of simply supported functionally graded rectangular plates using three-dimensional theory of elasticity. Ferreira et al. [8] studied the free vibration of functionally graded rectangular plates using first and third-order shear deformation plate theories by employing a mesh-less method. Matsunaga [9] presented the Navier solution for free vibration and stability of rectangular plates made of functionally graded materials according to a 2D higher-order deformation theory. Hasani Baferani et al. [10] used Reddy's third-order shear deformation theory to investigate the free vibration of thick functionally graded rectangular plates resting on elastic foundation. They also studied the effects of in-plane displacements on the system's response. Jin et al. [11] presented an exact solution for free vibrations of thick functionally graded rectangular plates by employing Rayleigh-Ritz procedure on the basis of three-dimensional theory of elasticity.

In recent years, smart materials such as piezoelectric materials have been proposed to control vibrations. Due to the coupling between electric and mechanical fields, piezoelectric materials can be used in a wide variety of applications including sensors and actuators. Few studies have been performed to investigate the vibration of plates surrounded by piezoelectric layers. For example, Huang et al. [12] investigated the vibration control of a laminated plate with piezoelectric layers using finite element method based on classical plate theory. Heyliger and Saravanos [13] presented an exact solution for the free vibration of simply supported laminated plates with embedded piezoelectric layers. Liang and Batra [14] studied changes in frequencies of a coupled laminated plate due to the presence of piezoelectric layers. In their paper, they investigated the effects of thickness, mass density and stiffness of piezoelectric layers on the natural frequency of a plate with simply supported edges. He et al. [15] carried out the active control of FGM plates integrated with piezoelectric sensors and actuators under various boundary conditions using finite element method. Baillargeon and vel [16] presented an exact solution for vibration of simply supported laminated composite plates with embedded piezoelectric shear actuators based on 3D theory of elasticity. Vibration analysis of simply supported composite plate containing piezoelectric layers was considered by Pietrzakowski [17] based on the Kirchhoff hypothesis and Mindlin plate theory. Askari Farsangi and Saidi [18] presented an analytical solution for free vibration of functionally graded rectangular plates with piezoelectric layers by using Mindlin plate theory. Askari Farsangi et al. [19] proposed an exact solution for free vibration of moderately thick hybrid

piezoelectric laminated plates under Levy-type boundary conditions according to first-order shear deformation theory.

Despite various studies on rectangular plates made of homogeneous, isotropic, piezoelectric and functionally graded materials, there are few studies dealing with the mechanical behavior of porous structures. Theodorakopoulos and Beskos [20] studied the flexural vibration of a simply supported thin rectangular plates made of fluid-saturated poroelastic materials by using classical plate theory. Leclaire et al. [21] investigated the transverse vibrations of a thin homogenous rectangular porous plate saturated by a fluid according to CPT. Magnucka-Blandzi [22-23] carried out the vibrational behavior, deflection and buckling of a porous-cellular circular plate using a nonlinear deformation theory. In her works, the distribution of mechanical properties along the plate thickness is considered to be symmetrical relative to the middle plane of plate. Khorshidvand et al. [24] investigated the buckling analysis of a clamped porous circular plate with piezoelectric layers based on classical plate theory. Rezaei and Saidi [25] presented an exact solution for the free vibration analysis of thick rectangular plates made of rigid porous materials saturated by inviscid fluid according to the Reddy's third-order shear deformation plate theory with Levy-type boundary conditions. The effect of porosity on natural frequencies of thick porous-cellular plates has been studied by Rezaei and Saidi [26] on the basis of Carrera Unified Formulation.

In this study, free vibration analysis of thick rectangular plates made of porous-cellular materials with piezoelectric layers has been investigated based on the Reddy's third-order shear deformation plate theory. Material properties of porous plate vary through its thickness based on a cosine rule. Using Hamilton's principle and Maxwell equation, governing equations for open and closed circuit electrical boundary conditions have been obtained. Then, an exact solution has been presented and numerical results for various electrical and mechanical boundary conditions have been obtained. Finally, the effect of geometric parameters as well as stiffness and electrical effects of piezoelectric layers on the natural frequency of the plate have been studied in detail.

2. Kinematic assumptions

Consider a rectangular plate of length a , width b , thickness of the porous core $2h$ and each piezoelectric layer h_p . x_1 and x_2 are in plane coordinates and x_3 is the coordinate in thickness direction. The geometry of the plate as well as its coordinate system may be seen in Fig. 1. As can be seen in Fig. 1, the origin of coordinate system is located at the mid-plane of the plate.

Based on third-order shear deformation theory, the displacement field is [2]

$$\begin{aligned}
 u_1(x_1, x_2, x_3, t) &= u(x_1, x_2, t) + x_3 \psi_1(x_1, x_2, t) - \alpha x_3^3 \left(\psi_1(x_1, x_2, t) + \frac{\partial w(x_1, x_2, t)}{\partial x_1} \right) \\
 u_2(x_1, x_2, x_3, t) &= v(x_1, x_2, t) + x_3 \psi_2(x_1, x_2, t) - \alpha x_3^3 \left(\psi_2(x_1, x_2, t) + \frac{\partial w(x_1, x_2, t)}{\partial x_2} \right) \\
 u_3(x_1, x_2, x_3, t) &= w(x_1, x_2, t)
 \end{aligned} \tag{1}$$

where the functions u_1 , u_2 and u_3 represent the components of displacement field in x_1 , x_2 and x_3 directions, respectively. u and v are the in-plane displacements in the x_1 and x_2 directions, respectively. w represents the transverse displacement of the middle plane. Also, ψ_1 and ψ_2 denote the rotations of the line perpendicular to the mid-plane about x_2 and x_1 axes, respectively. t is the time variable and the constant α is equal to $4/[3(2h + 2h_p)^2]$.

3. Constitutive relations

3.1. Porous materials

Due to the non-uniform distribution of porosity in the structure of porous materials, different rules may be used to model the variation of mechanical properties. Properties of porous material are considered to be asymmetric with respect to mid-plane as follow [25]

$$\begin{aligned} E(x_3) &= E^{top} \left[1 - e_0 \cos \left(\frac{\pi(x_3 + h)}{4h} \right) \right] \\ \rho(x_3) &= \rho^{top} \left[1 - e_m \cos \left(\frac{\pi(x_3 + h)}{4h} \right) \right] \\ e_0 &= 1 - \frac{E^{bot}}{E^{top}} \quad , \quad e_m = 1 - \sqrt{1 - e_0} \end{aligned} \quad (2)$$

In the above equations, E and ρ represent the elastic modulus and the mass density of plate, respectively and the dimensionless parameter e_0 , ($0 < e_0 < 1$) denotes the coefficient of plate porosity. It is worth to note that zero value for this parameter means there is no porosity in material's structure. The superscripts "top" and "bot" denote the top and bottom surfaces of the plate, respectively. Fig. 2 shows the distribution of the elastic modulus in the thickness direction. These relations indicate that the mechanical properties of the plate have its maximum and minimum values at the upper and lower planes, respectively.

The strain-stress relations for porous materials can be expressed as

$$\epsilon_{ij} = \frac{1 + \nu}{2} \sigma_{ij} - \frac{\nu}{E} \sigma_{kk} \delta_{ij} \quad (3)$$

where, ϵ_{ij} , σ_{ij} , δ and ν are the strain components, stress components, Kronecker delta and Poisson's ratio, respectively. The above constitutive relations are in fact the reduced form the Biot's poroelastic constitutive law which is proposed to model the behavior of porous medium [26]. The relations are valid in a case in which the pore pressure is either very low or nonexistent. Assuming air or low pressure gas as fluid, it is reasonable to disregard the last term in Biot's constitutive relations. This assumption leads to Eq. (3) meaning that the effect of coupled solid-fluid deformation is negligible. It is convenient to classify porous metals into the type of materials which follow the above relations. Different studies [22- 23] have already used the assumption to investigate the static and dynamic analyses of porous-cellular plates. By assuming $\sigma_{33} = 0$, Eq. (3) may be rewritten as follows

$$\sigma_{11} = Q_{11}\epsilon_{11} + Q_{12}\epsilon_{22} \quad (4)$$

$$\begin{aligned}\sigma_{22} &= Q_{21}\varepsilon_{11} + Q_{11}\varepsilon_{22} \\ \sigma_{23} &= 2Q_{66}\varepsilon_{23} \\ \sigma_{13} &= 2Q_{66}\varepsilon_{13} \\ \sigma_{12} &= 2Q_{66}\varepsilon_{12}\end{aligned}$$

In which the coefficients Q_{ij} may be obtained from relations (A.1) of the Appendix.

3.2. Piezoelectric materials

Due to coupling between electrical and mechanical fields, the constitutive relations of piezoelectric materials are expressed as a combination of electrical and mechanical characteristics. The constitutive relations for linear piezoelectric materials are as follows [27]

$$T_i = c_{ij}S_j - e_{ki}E_k \quad i, j = 1, 2, 3, 4, 5, 6 \quad (5.a)$$

$$D_k = e_{kj}S_j + \Xi_{km}E_m \quad m, k = 1, 2, 3 \quad (5.b)$$

where the vectors $\{D\}$ and $\{E\}$ represent the electrical displacement and field vectors, respectively. c_{ij} , Ξ_{km} And e_{ki} are the components of the piezoelectric stiffness, dielectric constants and piezoelectric coefficients matrices, respectively. Also, the components of T_i and S_j may be obtained as [27]

$$\begin{aligned}T_1 &= \sigma_{11} \quad , T_2 = \sigma_{22} \quad , T_3 = \sigma_{33} \quad , T_4 = \sigma_{23} \quad , T_5 = \sigma_{13} \quad , T_6 = \sigma_{12} \\ S_1 &= \varepsilon_{11} \quad , S_2 = \varepsilon_{22} \quad , S_3 = \varepsilon_{33} \quad , S_4 = 2\varepsilon_{23} \quad , S_5 = 2\varepsilon_{13} \quad , S_6 = 2\varepsilon_{12}\end{aligned} \quad (6)$$

Transversely isotropic piezoelectric materials have been considered in this study being a type of piezoelectrics which is polarized in the thickness direction. Considering $\sigma_{33} = 0$, Eqs. (5) can be expressed as

$$\begin{aligned}\sigma_{11} &= \bar{c}_{11}\varepsilon_{11} + \bar{c}_{12}\varepsilon_{22} - \bar{e}_{31}E_3 \\ \sigma_{22} &= \bar{c}_{12}\varepsilon_{11} + \bar{c}_{11}\varepsilon_{22} - \bar{e}_{31}E_3 \\ \sigma_{23} &= 2c_{55}\varepsilon_{23} - e_{15}E_2 \\ \sigma_{13} &= 2c_{55}\varepsilon_{13} - e_{15}E_1 \\ \sigma_{12} &= (\bar{c}_{11} - \bar{c}_{12})\varepsilon_{12}\end{aligned} \quad (7.a)$$

$$\begin{aligned}D_1 &= 2e_{15}\varepsilon_{13} + \Xi_{11}E_1 \\ D_2 &= 2e_{15}\varepsilon_{23} + \Xi_{11}E_2 \\ D_3 &= \bar{e}_{31}(\varepsilon_{11} + \varepsilon_{22}) + \bar{\Xi}_{33}E_3\end{aligned} \quad (7.b)$$

Here \bar{c}_{11} , \bar{c}_{12} , \bar{e}_{31} and $\bar{\Xi}_{33}$ are reduced constants given as relations (A.2) in the Appendix.

4. Mechanical and electrical fields

The components of the strain tensor in Cartesian coordinates are as follow

$$\varepsilon_{ij} = \frac{1}{2} \left(\frac{\partial u_i}{\partial x_j} + \frac{\partial u_j}{\partial x_i} \right) \quad (8)$$

By substituting the displacement field in Eq. (8), the components of the strain tensor are obtained as

$$\begin{aligned}
 \varepsilon_{11} &= \frac{\partial u}{\partial x_1} + x_3 \frac{\partial \psi_1}{\partial x_1} - \alpha x_3^3 \left(\frac{\partial \psi_1}{\partial x_1} + \frac{\partial^2 w}{\partial x_1^2} \right) \\
 \varepsilon_{22} &= \frac{\partial v}{\partial x_2} + x_3 \frac{\partial \psi_2}{\partial x_2} - \alpha x_3^3 \left(\frac{\partial \psi_2}{\partial x_2} + \frac{\partial^2 w}{\partial x_2^2} \right) \\
 \varepsilon_{33} &= 0 \\
 2\varepsilon_{12} &= \frac{\partial u}{\partial x_2} + \frac{\partial v}{\partial x_1} + x_3 \left(\frac{\partial \psi_1}{\partial x_2} + \frac{\partial \psi_2}{\partial x_1} \right) - \alpha x_3^3 \left(\frac{\partial \psi_1}{\partial x_2} + \frac{\partial \psi_2}{\partial x_1} + 2 \frac{\partial^2 w}{\partial x_1 \partial x_2} \right) \\
 2\varepsilon_{13} &= (1 - \beta x_3^2) \left(\psi_1 + \frac{\partial w}{\partial x_1} \right) \\
 2\varepsilon_{23} &= (1 - \beta x_3^2) \left(\psi_2 + \frac{\partial w}{\partial x_2} \right)
 \end{aligned} \tag{9}$$

where

$$\beta = 3\alpha = \frac{4}{(2h + 2h_p)^2} \tag{10}$$

Based on Eqs. (9), it can be seen that the shear strain components are not constant in the thickness direction due to using TSDT, unlike first-order shear deformation plate theory.

4.1. Closed circuit condition

In this case, the electrodes on the upper and lower surfaces of the piezoelectric coupled plate are connected to each other. Electric potential function for closed circuit condition is considered as follows [28]

$$\Phi(x_1, x_2, x_3, t) = \begin{cases} \phi(x_1, x_2, t) \left[1 - \left(\frac{x_3 - h - h_p/2}{h_p/2} \right)^2 \right] & (h \leq x_3 \leq h + h_p) \\ \phi(x_1, x_2, t) \left[1 - \left(\frac{-x_3 - h - h_p/2}{h_p/2} \right)^2 \right] & (-h - h_p \leq x_3 \leq -h) \end{cases} \tag{11}$$

Here, $\phi(x_1, x_2, t)$ denotes the electric potential in the mid-surface of piezoelectric layers. Eq. (11) implies that the electric potential of major surfaces of the piezoelectric layer is zero and the maximum value occurs at mid-surface of each layer.

4.2. Open circuit condition

Provided that the outer surface of the piezoelectric layer is exposed to an environment with very low permeability (such as air or vacuum), the plate is under open circuit electrical boundary condition. Piezoelectric materials in this mode may be used in design tools such as

sensors and vibration absorbers. In this case, the electrical boundary conditions is as follows [29]

$$\begin{aligned} \text{at } x_3 = \pm(h) : \Phi &= 0 \\ \text{at } x_3 = \pm(h + h_p) D_3 &= 0 \end{aligned} \quad (12)$$

Similar to the closed state, the electric potential may be considered as

$$\Phi(x_1, x_2, x_3, t) = \begin{cases} \phi(x_1, x_2, t) \left[1 - \left(\frac{x_3 - h - h_p/2}{h_p/2} \right)^2 \right] + X & (h \leq x_3 \leq h + h_p) \\ \phi(x_1, x_2, t) \left[1 - \left(\frac{-x_3 - h - h_p/2}{h_p/2} \right)^2 \right] + X' & (-h - h_p \leq x_3 \leq -h) \end{cases} \quad (13)$$

where X and X' are linear functions of the thickness coordinate as $X = Ax_3 + B$ and $X' = A'x_3 + B'$. By satisfying the electrical boundary conditions in Eqs. (12), the unknown parameters A, B, A' and B' may be obtained. These parameters are given as relations (A.3) of the Appendix. On the other hand, the electric potential distribution, Φ in piezoelectric layer is considered as a second-order function in the thickness direction.

Further, the electric field (\vec{E}) could be obtained as follow [30]

$$\vec{E} = -\vec{\nabla}\Phi = -\left(\frac{\partial\Phi}{\partial x_1} \vec{e}_1 + \frac{\partial\Phi}{\partial x_2} \vec{e}_2 + \frac{\partial\Phi}{\partial x_3} \vec{e}_3 \right) \quad (14)$$

5. Governing equations

5.1. Obtained equations from Hamilton's principle

Using Hamilton's principle, the equations of motion may be derived as

$$\delta u: \quad \frac{\partial N_{11}}{\partial x_1} + \frac{\partial N_{12}}{\partial x_2} = I_0 \frac{\partial^2 u}{\partial t^2} + I_1 \frac{\partial^2 \psi_1}{\partial t^2} - \alpha I_3 \left(\frac{\partial^2 \psi_1}{\partial t^2} + \frac{\partial^3 w}{\partial x_1 \partial t^2} \right) \quad (15.a)$$

$$\delta v: \quad \frac{\partial N_{12}}{\partial x_1} + \frac{\partial N_{22}}{\partial x_2} = I_0 \frac{\partial^2 v}{\partial t^2} + I_1 \frac{\partial^2 \psi_2}{\partial t^2} - \alpha I_3 \left(\frac{\partial^2 \psi_2}{\partial t^2} + \frac{\partial^3 w}{\partial x_2 \partial t^2} \right) \quad (15.b)$$

$$\begin{aligned} \delta \psi_1: \quad \frac{\partial M_{11}}{\partial x_1} + \frac{\partial M_{12}}{\partial x_2} - \alpha \left(\frac{\partial P_{11}}{\partial x_1} + \frac{\partial P_{12}}{\partial x_2} \right) - Q_1 + \beta R_1 \\ = J_1 \frac{\partial^2 u}{\partial t^2} + J_2 \frac{\partial^2 \psi_1}{\partial t^2} - \alpha J_4 \left(\frac{\partial^2 \psi_1}{\partial t^2} + \frac{\partial^3 w}{\partial x_1 \partial t^2} \right) \end{aligned} \quad (15.c)$$

$$\begin{aligned} \delta \psi_2: \quad \frac{\partial M_{12}}{\partial x_1} + \frac{\partial M_{22}}{\partial x_2} - \alpha \left(\frac{\partial P_{12}}{\partial x_1} + \frac{\partial P_{22}}{\partial x_2} \right) - Q_2 + \beta R_2 \\ = J_1 \frac{\partial^2 v}{\partial t^2} + J_2 \frac{\partial^2 \psi_2}{\partial t^2} - \alpha J_4 \left(\frac{\partial^2 \psi_2}{\partial t^2} + \frac{\partial^3 w}{\partial x_2 \partial t^2} \right) \end{aligned} \quad (15.d)$$

$$\begin{aligned}
\delta w: \quad & \frac{\partial Q_1}{\partial x_1} + \frac{\partial Q_2}{\partial x_2} - \beta \left(\frac{\partial R_1}{\partial x_1} + \frac{\partial R_2}{\partial x_2} \right) + \alpha \left(\frac{\partial^2 P_{11}}{\partial x_1^2} + 2 \frac{\partial^2 P_{12}}{\partial x_1 \partial x_2} + \frac{\partial^2 P_{22}}{\partial x_2^2} \right) \\
& = I_0 \frac{\partial^2 w}{\partial t^2} + \alpha I_3 \left(\frac{\partial^3 u}{\partial x_1 \partial t^2} + \frac{\partial^3 v}{\partial x_2 \partial t^2} \right) + \alpha I_4 \left(\frac{\partial^3 \psi_1}{\partial x_1 \partial t^2} + \frac{\partial^3 \psi_2}{\partial x_2 \partial t^2} \right) \\
& - \alpha^2 I_6 \left(\frac{\partial^3 \psi_1}{\partial x_1 \partial t^2} + \frac{\partial^3 \psi_2}{\partial x_2 \partial t^2} + \frac{\partial^4 w}{\partial x_1^2 \partial t^2} + \frac{\partial^4 w}{\partial x_2^2 \partial t^2} \right)
\end{aligned} \tag{15.e}$$

In the above, the stress resultants and the inertia terms are defined as follow

$$\begin{aligned}
\{N_{ij}, M_{ij}, P_{ij}\} &= \int_{-h-h_p}^{h+h_p} \sigma_{ij} \{1, x_3, x_3^3\} dx_3 \quad (i, j = 1, 2) \\
\{Q_k, R_k\} &= \int_{-h-h_p}^{h+h_p} \sigma_{k3} \{1, x_3^2\} dx_3 \quad (k = 1, 2) \\
I_m &= \int_{-h-h_p}^{h+h_p} \rho(x_3) x_3^m dx_3 \quad (m = 0, 1, 2, 3, 4, 6) \\
J_n &= I_n - \alpha I_{n+2} \quad (n = 1, 2, 4)
\end{aligned} \tag{16}$$

The stress resultants in terms of displacement components can be rewritten as

$$\begin{aligned}
N_{11} &= A_{11} \frac{\partial u}{\partial x_1} + A_{12} \frac{\partial v}{\partial x_2} + B_{11} \frac{\partial \psi_1}{\partial x_1} + B_{12} \frac{\partial \psi_2}{\partial x_2} - C_{11} \frac{\partial^2 w}{\partial x_1^2} - C_{12} \frac{\partial^2 w}{\partial x_2^2} \\
N_{22} &= A_{12} \frac{\partial u}{\partial x_1} + A_{11} \frac{\partial v}{\partial x_2} + B_{12} \frac{\partial \psi_1}{\partial x_1} + B_{11} \frac{\partial \psi_2}{\partial x_2} - C_{12} \frac{\partial^2 w}{\partial x_1^2} - C_{11} \frac{\partial^2 w}{\partial x_2^2} \\
N_{12} &= A_{66} \left(\frac{\partial u}{\partial x_2} + \frac{\partial v}{\partial x_1} \right) + B_{66} \left(\frac{\partial \psi_1}{\partial x_2} + \frac{\partial \psi_2}{\partial x_1} \right) - C_{66} \frac{\partial^2 w}{\partial x_1 \partial x_2} \\
M_{11} &= D_{11} \frac{\partial u}{\partial x_1} + D_{12} \frac{\partial v}{\partial x_2} + E_{11} \frac{\partial \psi_1}{\partial x_1} + E_{12} \frac{\partial \psi_2}{\partial x_2} - F_{11} \frac{\partial^2 w}{\partial x_1^2} - F_{12} \frac{\partial^2 w}{\partial x_2^2} - \tilde{\mu}_1 \phi \\
M_{22} &= D_{12} \frac{\partial u}{\partial x_1} + D_{11} \frac{\partial v}{\partial x_2} + E_{12} \frac{\partial \psi_1}{\partial x_1} + E_{11} \frac{\partial \psi_2}{\partial x_2} - F_{12} \frac{\partial^2 w}{\partial x_1^2} - F_{11} \frac{\partial^2 w}{\partial x_2^2} - \tilde{\mu}_1 \phi \\
M_{12} &= D_{66} \left(\frac{\partial u}{\partial x_2} + \frac{\partial v}{\partial x_1} \right) + E_{66} \left(\frac{\partial \psi_1}{\partial x_2} + \frac{\partial \psi_2}{\partial x_1} \right) - F_{66} \frac{\partial^2 w}{\partial x_1 \partial x_2} \\
Q_1 &= A_{55} \left(\psi_1 + \frac{\partial w}{\partial x_1} \right) + \tilde{\mu}_3 \frac{\partial \phi}{\partial x_1} + \bar{\mu}_1 \left(\frac{\partial^2 \psi_1}{\partial x_1^2} + \frac{\partial^2 \psi_2}{\partial x_1 \partial x_2} \right) + \bar{\mu}_3 \frac{\partial (\nabla^2 w)}{\partial x_1} \\
Q_2 &= A_{55} \left(\psi_2 + \frac{\partial w}{\partial x_2} \right) + \tilde{\mu}_3 \frac{\partial \phi}{\partial x_2} + \bar{\mu}_1 \left(\frac{\partial^2 \psi_1}{\partial x_1 \partial x_2} + \frac{\partial^2 \psi_2}{\partial x_2^2} \right) + \bar{\mu}_3 \frac{\partial (\nabla^2 w)}{\partial x_2} \\
P_{11} &= J_{11} \frac{\partial u}{\partial x_1} + J_{12} \frac{\partial v}{\partial x_2} + K_{11} \frac{\partial \psi_1}{\partial x_1} + K_{12} \frac{\partial \psi_2}{\partial x_2} - L_{11} \frac{\partial^2 w}{\partial x_1^2} - L_{12} \frac{\partial^2 w}{\partial x_2^2} - \tilde{\mu}_4 \phi \\
P_{22} &= J_{12} \frac{\partial u}{\partial x_1} + J_{11} \frac{\partial v}{\partial x_2} + K_{12} \frac{\partial \psi_1}{\partial x_1} + K_{11} \frac{\partial \psi_2}{\partial x_2} - L_{12} \frac{\partial^2 w}{\partial x_1^2} - L_{11} \frac{\partial^2 w}{\partial x_2^2} - \tilde{\mu}_4 \phi \\
P_{12} &= J_{66} \left(\frac{\partial u}{\partial x_2} + \frac{\partial v}{\partial x_1} \right) + K_{66} \left(\frac{\partial \psi_1}{\partial x_2} + \frac{\partial \psi_2}{\partial x_1} \right) - L_{66} \frac{\partial^2 w}{\partial x_1 \partial x_2}
\end{aligned} \tag{17}$$

$$R_1 = S_{55} \left(\psi_1 + \frac{\partial w}{\partial x_1} \right) + \tilde{\mu}_5 \frac{\partial \phi}{\partial x_1} + \bar{\mu}_4 \left(\frac{\partial^2 \psi_1}{\partial x_1^2} + \frac{\partial^2 \psi_2}{\partial x_1 \partial x_2} \right) + \bar{\mu}_5 \left(\frac{\partial(\nabla^2 w)}{\partial x_1} \right)$$

$$R_2 = S_{55} \left(\psi_2 + \frac{\partial w}{\partial x_2} \right) + \tilde{\mu}_5 \frac{\partial \phi}{\partial x_2} + \bar{\mu}_4 \left(\frac{\partial^2 \psi_1}{\partial x_1 \partial x_2} + \frac{\partial^2 \psi_2}{\partial x_2^2} \right) + \bar{\mu}_5 \left(\frac{\partial(\nabla^2 w)}{\partial x_2} \right)$$

The unknown constants in Eqs. (17) are given as Eqs. (A.4-A.6) of the Appendix. ∇^2 represents the Laplacian operator in 2D Cartesian coordinates. By substituting Eqs. (17) in the system of Eqs. (15), the governing equations of motion can be rewritten as

$$A_{11} \frac{\partial}{\partial x_1} \left(\frac{\partial u}{\partial x_1} + \frac{\partial v}{\partial x_2} \right) + A_{66} \frac{\partial}{\partial x_2} \left(\frac{\partial u}{\partial x_2} - \frac{\partial v}{\partial x_1} \right) + B_{11} \frac{\partial}{\partial x_1} \left(\frac{\partial \psi_1}{\partial x_1} + \frac{\partial \psi_2}{\partial x_2} \right) + B_{66} \frac{\partial}{\partial x_2} \left(\frac{\partial \psi_1}{\partial x_2} - \frac{\partial \psi_2}{\partial x_1} \right) - C_{11} \frac{\partial(\nabla^2 w)}{\partial x_1} = I_0 \frac{\partial^2 u}{\partial t^2} + I_1 \frac{\partial^2 \psi_1}{\partial t^2} - \alpha I_3 \left(\frac{\partial^2 \psi_1}{\partial t^2} + \frac{\partial^3 w}{\partial x_1 \partial t^2} \right) \quad (18.a)$$

$$A_{11} \frac{\partial}{\partial x_2} \left(\frac{\partial u}{\partial x_1} + \frac{\partial v}{\partial x_2} \right) - A_{66} \frac{\partial}{\partial x_1} \left(\frac{\partial u}{\partial x_2} - \frac{\partial v}{\partial x_1} \right) + B_{11} \frac{\partial}{\partial x_2} \left(\frac{\partial \psi_1}{\partial x_1} + \frac{\partial \psi_2}{\partial x_2} \right) - B_{66} \frac{\partial}{\partial x_1} \left(\frac{\partial \psi_1}{\partial x_2} - \frac{\partial \psi_2}{\partial x_1} \right) - C_{11} \frac{\partial(\nabla^2 w)}{\partial x_2} = I_0 \frac{\partial^2 v}{\partial t^2} + I_1 \frac{\partial^2 \psi_2}{\partial t^2} - \alpha I_3 \left(\frac{\partial^2 \psi_2}{\partial t^2} + \frac{\partial^3 w}{\partial x_2 \partial t^2} \right) \quad (18.b)$$

$$B_{11} \frac{\partial}{\partial x_1} \left(\frac{\partial u}{\partial x_1} + \frac{\partial v}{\partial x_2} \right) + B_{66} \frac{\partial}{\partial x_2} \left(\frac{\partial u}{\partial x_2} - \frac{\partial v}{\partial x_1} \right) + \hat{S}_1 \frac{\partial}{\partial x_1} \left(\frac{\partial \psi_1}{\partial x_1} + \frac{\partial \psi_2}{\partial x_2} \right) + X_{66} \frac{\partial}{\partial x_2} \left(\frac{\partial \psi_1}{\partial x_2} - \frac{\partial \psi_2}{\partial x_1} \right) + \hat{S}_2 \frac{\partial(\nabla^2 w)}{\partial x_1} + X_{55} \left(\psi_1 + \frac{\partial w}{\partial x_1} \right) + \hat{S}_3 \frac{\partial \phi}{\partial x_1} = J_1 \frac{\partial^2 u}{\partial t^2} + J_2 \frac{\partial^2 \psi_1}{\partial t^2} - \alpha J_4 \left(\frac{\partial^2 \psi_1}{\partial t^2} + \frac{\partial^3 w}{\partial x_1 \partial t^2} \right) \quad (18.c)$$

$$B_{11} \frac{\partial}{\partial x_2} \left(\frac{\partial u}{\partial x_1} + \frac{\partial v}{\partial x_2} \right) - B_{66} \frac{\partial}{\partial x_1} \left(\frac{\partial u}{\partial x_2} - \frac{\partial v}{\partial x_1} \right) + \hat{S}_1 \frac{\partial}{\partial x_2} \left(\frac{\partial \psi_1}{\partial x_1} + \frac{\partial \psi_2}{\partial x_2} \right) - X_{66} \frac{\partial}{\partial x_1} \left(\frac{\partial \psi_1}{\partial x_2} - \frac{\partial \psi_2}{\partial x_1} \right) + \hat{S}_2 \frac{\partial(\nabla^2 w)}{\partial x_2} + X_{55} \left(\psi_2 + \frac{\partial w}{\partial x_2} \right) + \hat{S}_3 \frac{\partial \phi}{\partial x_2} = J_1 \frac{\partial^2 v}{\partial t^2} + J_2 \frac{\partial^2 \psi_2}{\partial t^2} - \alpha J_4 \left(\frac{\partial^2 \psi_2}{\partial t^2} + \frac{\partial^3 w}{\partial x_2 \partial t^2} \right) \quad (18.d)$$

$$-X_{55} \left(\nabla^2 w + \frac{\partial \psi_1}{\partial x_1} + \frac{\partial \psi_2}{\partial x_2} \right) + \hat{S}_4 \nabla^2 \phi + \hat{S}_5 \left[\nabla^2 \left(\frac{\partial \psi_1}{\partial x_1} + \frac{\partial \psi_2}{\partial x_2} \right) \right] + \alpha J_{11} \left[\nabla^2 \left(\frac{\partial u}{\partial x_1} + \frac{\partial v}{\partial x_2} \right) \right] + \hat{S}_6 \nabla^4 w = I_0 \frac{\partial^2 w}{\partial t^2} + \alpha I_3 \left[\frac{\partial^2}{\partial t^2} \left(\frac{\partial u}{\partial x_1} + \frac{\partial v}{\partial x_2} \right) \right] + (\alpha I_4 - \alpha^2 I_6) \left[\frac{\partial^2}{\partial t^2} \left(\frac{\partial \psi_1}{\partial x_1} + \frac{\partial \psi_2}{\partial x_2} \right) \right] - \alpha^2 I_6 \frac{\partial(\nabla^2 w)}{\partial t^2} \quad (18.e)$$

Here the unknown constants X_{55} , X_{66} and \hat{S}_i ($i = 1, 2, \dots, 6$) may be found from Eqs. (A.7) of the Appendix.

5.2. Maxwell equation

Maxwell equation may be expressed as follows [29]

$$\int_{-h-h_p}^{-h} \vec{\nabla} \cdot \vec{D} dx_3 + \int_h^{h+h_p} \vec{\nabla} \cdot \vec{D} dx_3 = 0 \quad (19)$$

By substituting Eqs. (7.b) and Eqs. (9) in Eq. (19), Maxwell equation takes the form

$$\mu_1 \left(\frac{\partial \psi_1}{\partial x_1} + \frac{\partial \psi_2}{\partial x_2} \right) + \mu_2 \nabla^2 w + \mu_3 \phi + \tilde{\mu}_2 \nabla^2 \phi + \bar{\mu}_2 \left[\nabla^2 \left(\frac{\partial \psi_1}{\partial x_1} + \frac{\partial \psi_2}{\partial x_2} \right) \right] + \bar{\mu}_6 \nabla^4 w = 0 \quad (20)$$

The unknown constants in the above equation are given in Eqs. (A.8-A.10) of the Appendix. Eqs. (18) and Eq. (20) form a highly coupled system of partial differential equations that cannot be solved analytically directly.

5.3. Decoupling procedure

In order to decouple the governing equations of motion, four auxiliary functions are assumed as

$$\phi_1 = \frac{\partial u}{\partial x_1} + \frac{\partial v}{\partial x_2}, \quad \phi_2 = \frac{\partial u}{\partial x_2} - \frac{\partial v}{\partial x_1}, \quad \phi_3 = \frac{\partial \psi_1}{\partial x_1} + \frac{\partial \psi_2}{\partial x_2}, \quad \phi_4 = \frac{\partial \psi_1}{\partial x_2} - \frac{\partial \psi_2}{\partial x_1} \quad (21)$$

By rewriting Eqs. (18) and Eq. (20) in terms of the auxiliary functions, the governing equations of motion are presented as follows

$$\begin{aligned} A_{11} \frac{\partial \phi_1}{\partial x_1} + A_{66} \frac{\partial \phi_2}{\partial x_2} + B_{11} \frac{\partial \phi_3}{\partial x_1} + B_{66} \frac{\partial \phi_4}{\partial x_2} - C_{11} \frac{\partial (\nabla^2 w)}{\partial x_1} \\ = I_0 \frac{\partial^2 u}{\partial t^2} + I_1 \frac{\partial^2 \psi_1}{\partial t^2} - \alpha I_3 \left(\frac{\partial^2 \psi_1}{\partial t^2} + \frac{\partial^3 w}{\partial x_1 \partial t^2} \right) \end{aligned} \quad (22.a)$$

$$\begin{aligned} A_{11} \frac{\partial \phi_1}{\partial x_2} - A_{66} \frac{\partial \phi_2}{\partial x_1} + B_{11} \frac{\partial \phi_3}{\partial x_2} - B_{66} \frac{\partial \phi_4}{\partial x_1} - C_{11} \frac{\partial (\nabla^2 w)}{\partial x_2} \\ = I_0 \frac{\partial^2 v}{\partial t^2} + I_1 \frac{\partial^2 \psi_2}{\partial t^2} - \alpha I_3 \left(\frac{\partial^2 \psi_2}{\partial t^2} + \frac{\partial^3 w}{\partial x_2 \partial t^2} \right) \end{aligned} \quad (22.b)$$

$$\begin{aligned} B_{11} \frac{\partial \phi_1}{\partial x_1} + B_{66} \frac{\partial \phi_2}{\partial x_2} + \hat{S}_1 \frac{\partial \phi_3}{\partial x_1} + X_{66} \frac{\partial \phi_4}{\partial x_2} + \hat{S}_2 \frac{\partial (\nabla^2 w)}{\partial x_1} + X_{55} \left(\psi_1 + \frac{\partial w}{\partial x_1} \right) + \hat{S}_3 \frac{\partial \phi}{\partial x_1} \\ = J_1 \frac{\partial^2 u}{\partial t^2} + J_2 \frac{\partial^2 \psi_1}{\partial t^2} - \alpha J_4 \left(\frac{\partial^2 \psi_1}{\partial t^2} + \frac{\partial^3 w}{\partial x_1 \partial t^2} \right) \end{aligned} \quad (22.c)$$

$$\begin{aligned} B_{11} \frac{\partial \phi_1}{\partial x_2} - B_{66} \frac{\partial \phi_2}{\partial x_1} + \hat{S}_1 \frac{\partial \phi_3}{\partial x_2} - X_{66} \frac{\partial \phi_4}{\partial x_1} + \hat{S}_2 \frac{\partial (\nabla^2 w)}{\partial x_2} + X_{55} \left(\psi_2 + \frac{\partial w}{\partial x_2} \right) + \hat{S}_3 \frac{\partial \phi}{\partial x_2} \\ = J_1 \frac{\partial^2 v}{\partial t^2} + J_2 \frac{\partial^2 \psi_2}{\partial t^2} - \alpha J_4 \left(\frac{\partial^2 \psi_2}{\partial t^2} + \frac{\partial^3 w}{\partial x_2 \partial t^2} \right) \end{aligned} \quad (22.d)$$

$$\begin{aligned} -X_{55} (\nabla^2 w + \phi_3) + \hat{S}_4 \nabla^2 \phi + \hat{S}_5 \nabla^2 \phi_3 + \alpha J_{11} \nabla^2 \phi_1 + \hat{S}_6 \nabla^4 w \\ = I_0 \frac{\partial^2 w}{\partial t^2} + \alpha I_3 \frac{\partial^2 \phi_1}{\partial t^2} + (\alpha I_4 - \alpha^2 I_6) \frac{\partial^2 \phi_3}{\partial t^2} - \alpha^2 I_6 \frac{\partial^2 (\nabla^2 w)}{\partial t^2} \end{aligned} \quad (22.e)$$

$$\mu_1\phi_3 + \mu_2\nabla^2 w + \mu_3\phi + \tilde{\mu}_2\nabla^2\phi + \bar{\mu}_2\nabla^2\phi_3 + \bar{\mu}_6\nabla^4 w = 0 \quad (22.f)$$

By differentiating Eqs. (22.a-22.d) with respect to in-plane coordinates and doing some algebraic manipulations, this system of equations takes the form

$$A_{11}\nabla^2\phi_1 + B_{11}\nabla^2\phi_3 - C_{11}\nabla^4 w = I_0 \frac{\partial^2\phi_1}{\partial t^2} + I_1 \frac{\partial^2\phi_3}{\partial t^2} - \alpha I_3 \left(\frac{\partial^2\phi_3}{\partial t^2} + \frac{\partial^2(\nabla^2 w)}{\partial t^2} \right) \quad (23.a)$$

$$B_{11}\nabla^2\phi_1 + \hat{S}_1\nabla^2\phi_3 + \hat{S}_2\nabla^4 w + X_{55}(\nabla^2 w + \phi_3) + \hat{S}_3\nabla^2\phi \\ = J_1 \frac{\partial^2\phi_1}{\partial t^2} + (J_2 - \alpha J_4) \frac{\partial^2\phi_3}{\partial t^2} - \alpha J_4 \frac{\partial^2(\nabla^2 w)}{\partial t^2} \quad (23.b)$$

$$A_{66}\nabla^2\phi_2 + B_{66}\nabla^2\phi_4 = I_0 \frac{\partial^2\phi_2}{\partial t^2} + J_1 \frac{\partial^2\phi_4}{\partial t^2} \quad (23.c)$$

$$B_{66}\nabla^2\phi_2 + X_{66}\nabla^2\phi_4 + X_{55}\phi_4 = J_1 \frac{\partial^2\phi_2}{\partial t^2} + (J_2 - \alpha J_4) \frac{\partial^2\phi_4}{\partial t^2} \quad (23.d)$$

$$-X_{55}(\phi_3 + \nabla^2 w) + \hat{S}_4\nabla^2\phi + \hat{S}_5\nabla^2\phi_3 + \alpha J_{11}\nabla^2\phi_1 + \hat{S}_6\nabla^4 w \\ = I_0 \frac{\partial^2 w}{\partial t^2} + \alpha I_3 \frac{\partial^2\phi_1}{\partial t^2} + (\alpha I_4 - \alpha^2 I_6) \frac{\partial^2\phi_3}{\partial t^2} - \alpha^2 I_6 \frac{\partial^2(\nabla^2 w)}{\partial t^2} \quad (23.e)$$

$$\mu_1\phi_3 + \mu_2\nabla^2 w + \mu_3\phi + \tilde{\mu}_2\nabla^2\phi + \bar{\mu}_2\nabla^2\phi_3 + \bar{\mu}_6\nabla^4 w = 0 \quad (23.f)$$

As can be seen, Eq. (23.a), Eq. (23.b), Eq. (23.e) and Eq. (23.f) contain two auxiliary functions; i.e., ϕ_1 and ϕ_3 , the electric potential function and transverse displacement of middle plane. On the other hand, Eq. (23.c) and Eq. (23.d) contain the remaining auxiliary functions; i.e., ϕ_2 and ϕ_4 . By assuming harmonic motion for the system, the unknown functions may be considered as

$$\begin{pmatrix} \phi_1(x_1, x_2, t) \\ \phi_2(x_1, x_2, t) \\ \phi_3(x_1, x_2, t) \\ \phi_4(x_1, x_2, t) \\ \phi(x_1, x_2, t) \\ w(x_1, x_2, t) \end{pmatrix} = \sum_{m=1}^{\infty} \begin{pmatrix} \phi_{1m}(x_1, x_2) \\ \phi_{2m}(x_1, x_2) \\ \phi_{3m}(x_1, x_2) \\ \phi_{4m}(x_1, x_2) \\ \phi_m(x_1, x_2) \\ w_m(x_1, x_2) \end{pmatrix} e^{i\omega_m t} \quad (24)$$

where ω_m is the natural frequency of the plate which has to be found. Then, by substituting Eqs. (24) in the system of Eqs. (23) and doing some algebraic calculations on the resulting system, the following equations can be obtained

$$\xi_1\nabla^{10}w_m + \xi_2\nabla^8 w_m + \xi_3\nabla^6 w_m + \xi_4\nabla^4 w_m + \xi_5\nabla^2 w_m + \xi_6 w_m = 0 \quad (25.a)$$

$$\phi_{3m} = \xi_7\nabla^8 w_m + \xi_8\nabla^6 w_m + \xi_9\nabla^4 w_m + \xi_{10}\nabla^2 w_m + \xi_{11}w_m \quad (25.b)$$

$$\phi_{1m} = Z_7\nabla^2\phi_{3m} + Z_8\nabla^4 w_m + Z_9\phi_{3m} + Z_{10}\nabla^2 w_m + Z_{11}w_m \quad (25.c)$$

$$\phi_m = Z_{12}\phi_{3m} + Z_{13}\nabla^2\phi_{3m} + Z_{14}\nabla^4 w_m + Z_{15}\nabla^2 w_m + Z_{16}w_m \quad (25.d)$$

$$\bar{\xi}_1\nabla^4\phi_{4m} + \bar{\xi}_2\nabla^2\phi_{4m} + \bar{\xi}_3\phi_{4m} = 0 \quad (25.e)$$

$$\phi_{2m} = \bar{\xi}_4\nabla^2\phi_{4m} + \bar{\xi}_5\phi_{4m} \quad (25.f)$$

The unknown coefficients in Eqs. (25) are given in relations (A.11) of the Appendix. As can be seen, by employing auxiliary functions, the governing equations of motion are reduced into two independent partial differential equations.

6. Levy-type solution

According to the Levy-type solution, two parallel edges are assumed to be simply supported (here at $x_1 = 0$ and $x_1 = a$), while arbitrary classical boundary conditions may be applied at other edges. In order to satisfy the final equations at simply supported edges, the function $w_m(x_1, x_2)$ and $\phi_{4m}(x_1, x_2)$ are considered as below

$$w_m(x_1, x_2) = \sum_{j=1}^{\infty} w_{mj}(x_2) \sin(\beta_j x_1) \quad , \quad \phi_{4m}(x_1, x_2) = \sum_{j=1}^{\infty} \phi_{4mj}(x_2) \cos(\beta_j x_1) \quad (26)$$

Here, $\beta_j = j\pi/a$ and j represents the number of half-waves in x_1 direction. By substituting Eqs. (26) in Eq. (25.a) and Eq. (25.e), the following equations may be obtained

$$\begin{aligned} \xi_1 \frac{d^{10} w_{mj}}{dx_2^{10}} + [-5\xi_1 \beta_j^2 + \xi_2] \frac{d^8 w_{mj}}{dx_2^8} + [10\xi_1 \beta_j^4 - 4\xi_2 \beta_j^2 + \xi_3] \frac{d^6 w_{mj}}{dx_2^6} \\ + [-10\xi_1 \beta_j^6 + 6\xi_2 \beta_j^4 - 3\xi_3 \beta_j^2 + \xi_4] \frac{d^4 w_{mj}}{dx_2^4} \\ + [5\xi_1 \beta_j^8 - 4\xi_2 \beta_j^6 + 3\xi_3 \beta_j^4 - 2\xi_4 \beta_j^2 + \xi_5] \frac{d^2 w_{mj}}{dx_2^2} \\ + [-\xi_1 \beta_j^{10} + \xi_2 \beta_j^8 - \xi_3 \beta_j^6 + \xi_4 \beta_j^4 - \xi_5 \beta_j^2 + \xi_6] w_{mj} = 0 \end{aligned} \quad (27.a)$$

$$\bar{\xi}_1 \frac{d^4 \phi_{4mj}}{dx_2^4} + [-2\bar{\xi}_1 \beta_j^2 + \bar{\xi}_2] \frac{d^2 \phi_{4mj}}{dx_2^2} + [\bar{\xi}_1 \beta_j^4 - \bar{\xi}_2 \beta_j^2 + \bar{\xi}_3] \phi_{4mj} = 0 \quad (27.b)$$

As can be seen, two homogeneous ordinary differential equations with constant coefficients have been obtained. General solution for the system of Eqs. (27) is as follow

$$\begin{aligned} w_{mj}(x_2) = \bar{C}_1 \sinh(\Omega_1 x_2) + \bar{C}_2 \cosh(\Omega_1 x_2) + \bar{C}_3 \sinh(\Omega_2 x_2) + \bar{C}_4 \cosh(\Omega_2 x_2) \\ + \bar{C}_5 \sinh(\Omega_3 x_2) + \bar{C}_6 \cosh(\Omega_3 x_2) \\ + \bar{C}_7 \sinh(\Omega_4 x_2) + \bar{C}_8 \cosh(\Omega_4 x_2) \\ + \bar{C}_9 \sinh(\Omega_5 x_2) + \bar{C}_{10} \cosh(\Omega_5 x_2) \end{aligned} \quad (28.a)$$

$$\begin{aligned} \phi_{4mj}(x_2) = \bar{C}_{11} \sinh(\bar{\Omega}_1 x_2) + \bar{C}_{12} \cosh(\bar{\Omega}_1 x_2) \\ + \bar{C}_{13} \sinh(\bar{\Omega}_2 x_2) + \bar{C}_{14} \cosh(\bar{\Omega}_2 x_2) \end{aligned} \quad (28.b)$$

where the coefficients $\bar{C}_i (i = 1, 2, \dots, 14)$ are unknown coefficients and the parameters $\Omega_k (k = 1, 2, 3, 4, 5)$ and $\bar{\Omega}_l (l = 1, 2)$ can be obtained by the following relations

$$\begin{aligned} \xi_1 \epsilon^5 + [-5\xi_1 \beta_j^2 + \xi_2] \epsilon^4 + [10\xi_1 \beta_j^4 - 4\xi_2 \beta_j^2 + \xi_3] \epsilon^3 \\ + [-10\xi_1 \beta_j^6 + 6\xi_2 \beta_j^4 - 3\xi_3 \beta_j^2 + \xi_4] \epsilon^2 \\ + [5\xi_1 \beta_j^8 - 4\xi_2 \beta_j^6 + 3\xi_3 \beta_j^4 - 2\xi_4 \beta_j^2 + \xi_5] \epsilon \\ + [-\xi_1 \beta_j^{10} + \xi_2 \beta_j^8 - \xi_3 \beta_j^6 + \xi_4 \beta_j^4 - \xi_5 \beta_j^2 + \xi_6] = 0 \end{aligned} \quad (29.a)$$

$$\bar{\xi}_1 \bar{\epsilon}^2 + [-2\bar{\xi}_1 \beta_j^2 + \bar{\xi}_2] \bar{\epsilon} + [\bar{\xi}_1 \beta_j^4 - \bar{\xi}_2 \beta_j^2 + \bar{\xi}_3] = 0 \quad (29.b)$$

where

$$\begin{aligned}\Omega_k &= \pm\sqrt{\epsilon_k} \\ \bar{\Omega}_l &= \pm\sqrt{\bar{\epsilon}_l}\end{aligned}\quad (30)$$

7. Boundary conditions

7.1. Electrical boundary conditions

Due to considering Levy-type solution, the electrical potential at simply supported edges is equal to zero; i.e.,

$$\begin{aligned}\text{at } x_1 = 0 : \phi &= 0 \\ \text{at } x_1 = a : \phi &= 0\end{aligned}\quad (31)$$

Also, the electrical boundary conditions at $x_2 = \pm b/2$ is as follow

$$\int_{-h-h_p}^{-h} D_2 \left(x_1, x_2 = \pm \frac{b}{2}, x_3, t \right) dx_3 + \int_h^{h+h_p} D_2 \left(x_1, x_2 = \pm \frac{b}{2}, x_3, t \right) dx_3 = 0 \quad (32)$$

By substituting D_2 from Eq. (7.b) in the above equation and using Eq. (9), electrical boundary conditions at $x_2 = \pm b/2$ can be obtained as

$$T_1 \left(\psi_2 + \frac{\partial w}{\partial x_2} \right) + \bar{T}_1 \frac{\partial \phi}{\partial x_2} + \bar{T}_1 \left(\frac{\partial^2 \psi_1}{\partial x_1 \partial x_2} + \frac{\partial^2 \psi_2}{\partial x_2^2} \right) + \bar{T}_2 \left[\frac{\partial}{\partial x_2} \left(\frac{\partial^2 w}{\partial x_1^2} + \frac{\partial^2 w}{\partial x_2^2} \right) \right] = 0 \quad (33)$$

Where the unknown coefficients in Eq. (33) are given as relations (A.12-14) of the Appendix.

7.2. Mechanical boundary conditions

Assuming that classical boundary conditions including free, clamped and simply supported which may be applied at $x_2 = \pm b/2$, the conditions for each types of boundary, are as follows

$$\begin{aligned}\text{(I) Free:} \quad N_{12} &= 0, N_{22} = 0, (M_{12} - \alpha P_{12}) = 0, (M_{22} - \alpha P_{22}) = \\ &0, P_{22} = 0 \\ Q_2 - \beta R_2 + \alpha \left(2 \frac{\partial P_{12}}{\partial x_1} + \frac{\partial P_{22}}{\partial x_2} \right) &= 0\end{aligned}\quad (34.a)$$

$$\text{(II) Clamped:} \quad u = 0, v = 0, \psi_1 = 0, \psi_2 = 0, w = 0, \frac{\partial w}{\partial x_2} = 0 \quad (34.b)$$

$$\text{(III) Simply supported:} \quad N_{22} = 0, u = 0, \psi_1 = 0, (M_{22} - \alpha P_{22}) = 0, w = 0, P_{22} = 0 \quad (34.c)$$

Finally, by applying electrical and mechanical boundary conditions at $x_2 = \pm b/2$, fourteen homogeneous algebraic equations in term of the unknown constants \bar{C}_i will be obtained. By equating the determinant of the coefficients of the fourteen equations to zero, the natural frequencies of the system can be determined.

8. Numerical results and discussion

The mechanical and electrical properties of different piezoelectric and porous-cellular materials are listed in table 1 [31].

For the sake of simplicity, the symbol $SXSY$ has been used to show the plate's boundary conditions that represents two parallel simply supported edges at $x_1 = 0$ and $x_2 = a$. Also, X and Y denote the type of boundary at the remaining edges. Symbols S , F and C represent simply supported, free, and clamped boundary conditions, respectively.

In order to verify the obtained results, frequencies have been compared with those available in literature for a simply supported homogeneous and isotropic square plate with $\rho = 5700 \text{ kg/m}^3$ and $E = 200 \text{ GPa}$ in table 2. Also, the Poisson's ratio is set to 0.3. The obtained frequencies are found to correlate well with the ones tabulated in other reference papers.

A comparative study has been performed to validate the obtained frequencies for a homogeneous and isotropic square plate under various boundary conditions in table 3. The results match well with those presented in literature; thus, the accuracy of the approach may be observed.

The first ten natural frequencies obtained from the present study for a simply supported homogeneous and isotropic plate bounded with piezoelectric layers with $2h/a = 1/80$ and $2h_p/a = 1/2000$ are compared with the finite element results of Ref. [15], Levy- type solution of Ref. [18] which is based on Mindlin plate theory and Navier solution of Ref. [32] in table 4. According to the frequencies listed in this table, it can be seen that the results predicted by CPT are slightly lower than the ones related to TSDT with maximum discrepancies of 3.07 %. It can also be observed that the results related to this theory are lower than that of FSDT [18] because third-order shear deformation theory considers plate to be softer. As seen, the comparison is well justified.

After establishing the correctness of the presented approach, numerical results for natural frequency response of porous rectangular plate made of cellular aluminum surrounded by layers of PZT-4 are presented for various geometric parameters under different electrical and mechanical boundary conditions.

To apply the proposed method to analyze piezoelectric coupled plates, Tables 5-7 show the effect of variation of core thickness and porosity on the lowest three natural frequencies of a square plate under Levy-type boundary conditions for both electrical boundary conditions. These tables reveals that by increasing the core thickness, natural frequency of various vibrational modes increases for all studied electrical and mechanical boundary conditions due to increasing in overall stiffness of the plate. Further, increasing the coefficient of plate porosity yields the decrease of the natural frequencies. In fact, the decrease in elastic modulus affects more prominently than that of mass density; therefore, the variation of mechanical properties leads to decrease in natural frequency. From the tables, it can also be found that, by imposing more constraints on the plate's edges causes natural frequencies to increase. In this regard, the lowest natural frequency belongs to a plate under SFSF boundary condition and the highest one is related to the similar plate under SCSC boundary condition.

In order to interpret the observed behaviors of natural frequency for both closed and open circuit piezoelectric layers, the fundamental natural frequency of a porous square plate

surrounded by piezoelectric layers under various classical boundary conditions, are listed in Table 8. Three piezoelectric coupled plates with thickness ratios given by 0.05, 0.1 and 0.2 are considered when the core thickness-length ratio is equal to 0.15. To present the effect of piezoelectric layers stiffness, frequencies listed in the third column are determined by disregarding piezo-effect; i.e., by equating the piezoelectric coefficients equal to zero ($e_{ij} = 0$) [29]. According to the data presented in this table, one can see that the piezo-effect in the closed circuit condition is negligible. The interesting point is that in case of open circuit condition, this effect plays a key role in increasing the natural frequency of piezoelectric coupled plates. This fact could be attributed to the different distributions of electric potential in thickness direction of the piezoelectric layers in these two cases. According to Eq. (11) and Eq. (13), it is clear that in closed circuit condition, the electric potential of the upper and lower surfaces of the layers is zero, while its maximum value occurs in the middle plane of each piezoelectric layer. On the other hand, in case of open circuit condition, the electric potential on adjacent surfaces of the core plate is zero and increases in the thickness direction of the piezoelectric layers so that it reaches its maximum value on the outer surface of the layers. In case of closed circuit condition, a large amount of electrical energy is released through electrodes; i.e., the decrease in effectiveness of piezo-effect causes the piezoelectric coupled plate stiffness to increase slightly. On the contrary, the electrical energy of the piezoelectric layers cannot be released while the plate is vibrating freely in the open circuit condition, which ultimately leads to increase in effective stiffness of the piezoelectric coupled plate and its natural frequency as well.

The first three natural frequencies of a porous plate coupled with piezoelectric layers under Levy-type boundary conditions for both closed and open circuit electrical boundary conditions are listed in table 9. Due to similar reason which has been stated above, the piezo-effect is much more significant in case of open circuit compared to closed circuit for all vibrational modes.

The variation of natural frequency due to the changes in aspect ratio for a porous plate coupled with piezoelectric layers under various mechanical boundary conditions is shown in Fig. 3. This figure indicates that by decreasing the width of the plate, the natural frequency increases for all studied boundary conditions except for *SFSF* boundary condition in which the natural frequency decreases slightly when the major surfaces of piezoelectric layers are held at zero voltage (closed circuit condition). It is observed that the natural frequencies of a plate with open circuit condition undertake similar changes versus aspect ratio.

So as to study the effect of piezoelectric layer, the natural frequency relative difference parameter is defined as follows

$$NFD = \frac{\omega_{pp} - \omega_p}{\omega_p} \quad (35)$$

where ω_{pp} is natural frequency of a piezoelectric coupled plate and ω_p denotes natural frequency of this plate in absence of piezoelectric layers. The variation of the natural frequency relative difference against the thickness ratio for various mechanical boundary

conditions for both closed and open circuit piezoelectric layers is depicted in Fig. 4. Due to positive NFD for all electrical and mechanical boundary conditions, it can be concluded that the natural frequency increases as piezoelectric layers are added to the core plate. In fact, the plate gets stiffer due to the presence of piezoelectric layers. This is because the flexural rigidity of piezoelectric layers is more considerable compared to the core plate; therefore, the piezoelectric coupled plate gets stiffer. On the other hand, the presence of piezoelectric layers increases the mass of the system which causes the natural frequency to decrease. By investigating the effect of piezoelectric layers on natural frequency of the system, it could be deduced that the effect of flexural rigidity of piezoelectric layers overcomes the effect of their mass density.

The variation of natural frequency relative difference versus $2h_p/a$ for a square piezoelectric coupled plate under SSSF and SSSS boundary conditions for different values of core thickness-length ratio are shown in Fig. 5. It is observed from the plots for a particular value of e_0 , as core thickness increases, the value of NFD decreases due to adding the piezoelectric layers. It is to be noted, the changes in NFD parameter are less dependent on the variation of thickness of core plate when it is under SSSF boundary condition than that of a simply supported one.

As a further insight into these eigenfrequencies, the variation of NFD parameter corresponding to fundamental vibrational mode versus the thickness ratio for different coefficients of plate porosity for both open and closed circuit conditions, is depicted in Fig. 6. According to this figure, for both closed and open circuits, the NFD parameter owns higher values for higher porosity coefficients, which means that the effect of piezoelectric layers on natural frequency is more prominent for core plates with higher coefficient of plate porosity.

Considering constant mass for a plate, the variation of fundamental natural frequency of a porous plate against the coefficient of plate porosity is shown in Fig. 7. Also, the effect of the same parameter on natural frequency when two piezoelectric layers are bonded on bottom and top surfaces of the plate is demonstrated in Fig. 8. It can be seen the natural frequency increases as the value of plate's thickness and its coefficient of plate porosity increase simultaneously (in such a way that the overall mass of the plate remains constant) under all studied electrical and mechanical boundary conditions. Therefore, the variation of plate's thickness does have greater effect on natural frequency of the plate compared to the coefficient of plate porosity. Moreover, the figures indicate that the graph related to a plate with integrated piezoelectric layers changes with steeper slope comparing with trends shown in Fig. 7. For example, as the coefficient of plate porosity vary from zero to 0.8, the natural frequency of a porous plate with constant mass under SSSF boundary condition increases by 18.8%, while the frequency increases by almost 34% for a piezoelectric coupled plate with same conditions for both open and closed circuits. As a further matter, it could be observed that the above mentioned point is more considerable for plates with softer mechanical boundary conditions.

9. Conclusion

In this study, third-order shear deformation plate theory has been employed to analyze the free vibration of porous plates coupled with piezoelectric layers. Using Hamilton's principle and Maxwell equation, the governing equations of motion have been obtained and solved analytically by using some auxiliary functions for Levy-type boundary conditions. The natural frequencies of the plate have been extracted for various geometric dimensions under different mechanical and electrical boundary conditions. The effects of plate porosity, geometric dimensions as well as mechanical and electrical boundary conditions on natural frequency response of the plate coupled with piezoelectric layers have been studied. According to the obtained numerical results, the following concluding points may be reported

- The natural frequency of plates decreases as the coefficient of plate porosity increases in all studied mechanical and electrical boundary conditions.
- In closed circuit condition, the effect of piezoelectric layers on the natural frequency is negligible while this effect plays a key role in the natural frequency changes for the case of open circuit condition.
- Adding piezoelectric layers causes the natural frequency to increase for all studied electrical and mechanical boundary conditions.
- The piezo-effect is more prominent for plates with higher porosity, lower thickness and softer boundary conditions.
- The natural frequency of plates increases as both the thickness of porous plate and its coefficient of plate porosity increase (in such a way that the overall mass of the plate remains constant) for all considered boundary conditions. This effect is more significant for plates bounded with piezoelectric layers.

Appendix

The parameters Q_{ij} are defined as

$$\begin{aligned} Q_{11} &= \frac{E(x_3)}{1-\nu^2} \\ Q_{12} = Q_{21} &= \frac{\nu E(x_3)}{1-\nu^2} \\ Q_{66} &= \frac{1}{2}(Q_{11} - Q_{12}) = \frac{E(x_3)}{2(1+\nu)} \end{aligned} \quad (\text{A.1})$$

The reduced constants of piezoelectric materials are defined as

$$\begin{aligned} \bar{c}_{11} &= c_{11} - \frac{c_{13}^2}{c_{33}}, \quad \bar{c}_{12} = c_{12} - \frac{c_{13}^2}{c_{33}} \\ \bar{e}_{31} &= e_{31} - \frac{c_{13}}{c_{33}} e_{33}, \quad \bar{\epsilon}_{33} = \epsilon_{33} + \frac{e_{33}^2}{c_{33}} \end{aligned} \quad (\text{A.2})$$

$$\begin{aligned} B = -Ah &= -\frac{\bar{e}_{31}h}{\bar{\epsilon}_{33}} \left\{ \frac{\partial u}{\partial x_1} + \frac{\partial v}{\partial x_2} + [h + h_p - \alpha(h + h_p)^3] \left(\frac{\partial \psi_1}{\partial x_1} + \frac{\partial \psi_2}{\partial x_2} \right) \right. \\ &\quad \left. - \alpha(h + h_p)^3 \nabla^2 w \right\} - \frac{4\phi h}{h_p} \end{aligned}$$

$$B' = A'h = \frac{\bar{e}_{31}h}{\bar{\epsilon}_{33}} \left\{ \frac{\partial u}{\partial x_1} + \frac{\partial v}{\partial x_2} - [h + h_p - \alpha(h + h_p)^3] \left(\frac{\partial \psi_1}{\partial x_1} + \frac{\partial \psi_2}{\partial x_2} \right) + \alpha(h + h_p)^3 \nabla^2 w \right\} - \frac{4\phi h}{h_p} \quad (\text{A.3})$$

Stiffness coefficients

$$\begin{aligned} \{A_{11}, A_{12}\} &= \int_{-h}^{+h} \{Q_{11}, Q_{12}\} dx_3 + 2 \int_h^{h+h_p} \{\bar{c}_{11}, \bar{c}_{12}\} dx_3 + \eta_1 \\ A_{66} &= \int_{-h}^{+h} Q_{66} dx_3 + \int_h^{h+h_p} (\bar{c}_{11} - \bar{c}_{12}) dx_3 \\ \{B_{11}, B_{12}, B_{66}\} &= \int_{-h}^{+h} \{Q_{11}, Q_{12}, Q_{66}\} (x_3 - \alpha x_3^3) dx_3 \\ \{C_{11}, C_{12}, C_{66}\} &= \int_{-h}^{+h} \{Q_{11}, Q_{12}, 2Q_{66}\} \alpha x_3^3 dx_3 \\ \{D_{11}, D_{12}, D_{66}\} &= \int_{-h}^{+h} \{Q_{11}, Q_{12}, Q_{66}\} x_3 dx_3 \\ \{E_{11}, E_{12}\} &= \int_{-h}^{+h} \{Q_{11}, Q_{12}\} (x_3^2 - \alpha x_3^4) dx_3 + 2 \int_h^{h+h_p} \{\bar{c}_{11}, \bar{c}_{12}\} (x_3^2 - \alpha x_3^4) dx_3 + \eta_2 \\ E_{66} &= \int_{-h}^{+h} Q_{66} (x_3^2 - \alpha x_3^4) dx_3 + \int_h^{h+h_p} (\bar{c}_{11} - \bar{c}_{12}) (x_3^2 - \alpha x_3^4) dx_3 \\ \{F_{11}, F_{12}\} &= \int_{-h}^{+h} \{Q_{11}, Q_{12}\} \alpha x_3^4 dx_3 + 2 \int_h^{h+h_p} \{\bar{c}_{11}, \bar{c}_{12}\} \alpha x_3^4 dx_3 + \eta_3 \\ F_{66} &= 2 \int_{-h}^{+h} Q_{66} \alpha x_3^4 dx_3 + 2 \int_h^{h+h_p} (\bar{c}_{11} - \bar{c}_{12}) \alpha x_3^4 dx_3 \\ A_{55} &= \int_{-h}^{+h} Q_{66} (1 - \beta x_3^2) dx_3 + 2 \int_h^{h+h_p} \bar{c}_{55} (1 - \beta x_3^2) dx_3 \\ \{U_{11}, J_{12}, J_{66}\} &= \int_{-h}^{+h} \{Q_{11}, Q_{12}, Q_{66}\} x_3^3 dx_3 \\ \{K_{11}, K_{12}\} &= \int_{-h}^{+h} \{Q_{11}, Q_{12}\} (x_3^4 - \alpha x_3^6) dx_3 + 2 \int_h^{h+h_p} \{\bar{c}_{11}, \bar{c}_{12}\} (x_3^4 - \alpha x_3^6) dx_3 + \eta_4 \\ K_{66} &= \int_{-h}^{+h} Q_{66} (x_3^4 - \alpha x_3^6) dx_3 + \int_h^{h+h_p} (\bar{c}_{11} - \bar{c}_{12}) (x_3^4 - \alpha x_3^6) dx_3 \\ \{L_{11}, L_{12}\} &= \int_{-h}^{+h} \{Q_{11}, Q_{12}\} \alpha x_3^6 dx_3 + 2 \int_h^{h+h_p} \{\bar{c}_{11}, \bar{c}_{12}\} \alpha x_3^6 dx_3 + \eta_5 \\ L_{66} &= 2 \int_{-h}^{+h} Q_{66} \alpha x_3^6 dx_3 + 2 \int_h^{h+h_p} (\bar{c}_{11} - \bar{c}_{12}) \alpha x_3^6 dx_3 \\ S_{55} &= \int_{-h}^{+h} Q_{66} (x_3^2 - \beta x_3^4) dx_3 + 2 \int_h^{h+h_p} \bar{c}_{55} (x_3^2 - \beta x_3^4) dx_3 \end{aligned} \quad (\text{A.4})$$

Where, for an open circuit piezoelectric layer, we have

$$\eta_1 = \frac{2\bar{e}_{31}^2 h_p}{\bar{\epsilon}_{33}}$$

$$\begin{aligned}
\eta_2 &= \frac{\bar{e}_{31}^2 h_p (2h + h_p) (h + h_p - \alpha(h + h_p)^3)}{\bar{\epsilon}_{33}} \\
\eta_3 &= \frac{\alpha \bar{e}_{31}^2 h_p (h + h_p)^3 (2h + h_p)}{\bar{\epsilon}_{33}} \\
\eta_4 &= \frac{\bar{e}_{31}^2 \left(2h^3 h_p + 3h^2 h_p^2 + 2h h_p^3 + \frac{1}{2} h_p^4 \right) (h + h_p - \alpha(h + h_p)^3)}{\bar{\epsilon}_{33}} \\
\eta_5 &= \frac{\alpha \bar{e}_{31}^2 (h + h_p)^3 \left(2h^3 h_p + 3h^2 h_p^2 + 2h h_p^3 + \frac{1}{2} h_p^4 \right)}{\bar{\epsilon}_{33}} \\
\bar{\mu}_1 &= \frac{\bar{e}_{31} e_{15} h_p^2 (h + h_p - \alpha(h + h_p)^3)}{\bar{\epsilon}_{33}} \\
\bar{\mu}_3 &= -\frac{\alpha \bar{e}_{31} e_{15} h_p^2 (h + h_p)^2}{\bar{\epsilon}_{33}} \\
\bar{\mu}_4 &= \frac{\bar{e}_{31} e_{15} \left(h^2 h_p^2 + \frac{4}{3} h h_p^3 + \frac{1}{2} h_p^4 \right) (h + h_p - \alpha(h + h_p)^3)}{\bar{\epsilon}_{33}} \\
\bar{\mu}_5 &= -\frac{\alpha \bar{e}_{31} e_{15} (h + h_p)^3 \left(h^2 h_p^2 + \frac{4}{3} h h_p^3 + \frac{1}{2} h_p^4 \right)}{\bar{\epsilon}_{33}} \\
\tilde{\mu}_1 &= -\frac{8}{3} \bar{e}_{31} (3h + h_p) \\
\tilde{\mu}_3 &= \frac{16}{3} e_{15} h_p \\
\tilde{\mu}_4 &= -\frac{8 \bar{e}_{31}}{h_p^2} \left(h^3 h_p^2 + h^2 h_p^3 + \frac{1}{2} h h_p^4 + \frac{1}{10} h_p^5 \right) \\
\tilde{\mu}_5 &= \frac{e_{15}}{h_p^2} \left(\frac{12}{5} h_p^5 + \frac{16}{3} h^2 h_p^3 + \frac{20}{3} h h_p^4 \right)
\end{aligned} \tag{A.5}$$

And for a closed circuit piezoelectric layer

$$\begin{aligned}
\eta_1 &= 0, \quad \eta_2 = 0, \quad \eta_3 = 0, \quad \eta_4 = 0, \quad \eta_5 = 0 \\
\bar{\mu}_1 &= 0, \quad \bar{\mu}_3 = 0, \quad \bar{\mu}_4 = 0, \quad \bar{\mu}_5 = 0 \\
\tilde{\mu}_1 &= -\frac{4}{3} \bar{e}_{31} h_p \\
\tilde{\mu}_3 &= -\frac{4}{3} e_{15} h_p \\
\tilde{\mu}_4 &= -\frac{2 \bar{e}_{31} h_p}{5} (10h^2 + 10h h_p + 3h_p^2) \\
\tilde{\mu}_5 &= -\frac{2 e_{15} h_p}{15} (10h^2 + 10h h_p + 3h_p^2)
\end{aligned} \tag{A.6}$$

$$\hat{S}_1 = E_{11} - \alpha K_{11} + \beta \bar{\mu}_4 - \bar{\mu}_1$$

$$\begin{aligned}
\hat{S}_2 &= \alpha L_{11} - F_{11} + \beta \bar{\mu}_5 - \bar{\mu}_3 \\
\hat{S}_3 &= \alpha \bar{\mu}_4 + \beta \bar{\mu}_5 - \bar{\mu}_1 - \bar{\mu}_3 \\
\hat{S}_4 &= \bar{\mu}_3 - \alpha \bar{\mu}_4 - \beta \bar{\mu}_5 \\
\hat{S}_5 &= \alpha K_{11} + \bar{\mu}_1 - \beta \bar{\mu}_4 \\
\hat{S}_6 &= \bar{\mu}_3 - \alpha L_{11} - \beta \bar{\mu}_5 \\
X_{55} &= \beta S_{55} - A_{55} \\
X_{66} &= E_{66} - \alpha K_{66}
\end{aligned} \tag{A.7}$$

$$\begin{aligned}
\mu_1 &= -2\beta(e_{15} + \bar{e}_{31}) \left(h^2 h_p + h_p^2 h + \frac{1}{3} h_p^3 \right) + 2h_p(e_{15} + \bar{e}_{31}) \\
\mu_2 &= -2\beta(e_{15} + \bar{e}_{31}) \left(h^2 h_p + h_p^2 h + \frac{1}{3} h_p^3 \right) + 2e_{15} h_p \\
\mu_3 &= \frac{16\bar{E}_{33}}{h_p}
\end{aligned} \tag{A.8}$$

For open circuit condition

$$\begin{aligned}
\bar{\mu}_2 &= \frac{\bar{e}_{31} \bar{E}_{11} h_p^2}{\bar{E}_{33}} (\alpha h^3 + 3\alpha h^2 h_p + 3\alpha h_p^2 h + \alpha h_p^3 - h - h_p) \\
\bar{\mu}_6 &= \frac{\alpha \bar{E}_{11} \bar{e}_{31} h_p^2}{\bar{E}_{33}} (h + h_p)^3 \\
\bar{\mu}_2 &= -\frac{16h_p \bar{E}_{11}}{3}
\end{aligned} \tag{A.9}$$

And for closed circuit condition

$$\bar{\mu}_2 = 0, \quad \bar{\mu}_6 = 0, \quad \bar{\mu}_2 = -\frac{4h_p \bar{E}_{11}}{3} \tag{A.10}$$

The coefficients $Z_i (i = 1, 2, \dots, 27)$, $\bar{Z}_j (j = 17, 18, \dots, 22)$, $\xi_k (k = 1, 2, \dots, 11)$ and $\bar{\xi}_l (l = 1, 2, \dots, 5)$ are defined as

$$\begin{aligned}
Z_1 &= -\frac{-X_{55} - \frac{\alpha J_{11} \omega_m^2 J_1}{A_{11}} + (\alpha I_4 - \alpha^2 I_6) \omega_m^2}{\hat{S}_4} \\
Z_2 &= -\frac{-\frac{\alpha J_{11} B_{11}}{A_{11}} + \hat{S}_5}{\hat{S}_4} \\
Z_3 &= -\frac{-\frac{\alpha J_{11} C_{11}}{A_{11}} + \hat{S}_6}{\hat{S}_4} \\
Z_4 &= -\frac{-X_{55} - \frac{\alpha^2 J_{11} \omega_m^2 I_3}{A_{11}} - \alpha^2 I_6 \omega_m^2}{\hat{S}_4}
\end{aligned}$$

$$Z_5 = -\frac{-\frac{\alpha J_{11} \omega_m^2 I_0}{A_{11}} + \alpha I_3 \omega_m^2}{\hat{S}_4}$$

$$Z_6 = -\frac{I_6 \omega_m^2}{\hat{S}_4}$$

$$Z_7 = -\frac{-\frac{B_{11}^2}{A_{11}} + \hat{S}_1 + \hat{S}_3 Z_2}{-\frac{B_{11} I_0 \omega_m^2}{A_{11}} + \hat{S}_3 Z_5 + J_1 \omega_m^2}$$

$$Z_8 = -\frac{\frac{B_{11} C_{11}}{A_{11}} + \hat{S}_2 + \hat{S}_3 Z_3}{-\frac{B_{11} I_0 \omega_m^2}{A_{11}} + \hat{S}_3 Z_5 + J_1 \omega_m^2}$$

$$Z_9 = -\frac{-\frac{B_{11} J_1 \omega_m^2}{A_{11}} + X_{55} + \hat{S}_3 Z_1 + (J_2 - \alpha J_4) \omega_m^2}{-\frac{B_{11} I_0 \omega_m^2}{A_{11}} + \hat{S}_3 Z_5 + J_1 \omega_m^2}$$

$$Z_{10} = -\frac{\frac{\alpha B_{11} I_3 \omega_m^2}{A_{11}} + X_{55} + \hat{S}_3 Z_4 - \alpha J_4 \omega_m^2}{-\frac{B_{11} I_0 \omega_m^2}{A_{11}} + \hat{S}_3 Z_5 + J_1 \omega_m^2}$$

$$Z_{11} = -\frac{\hat{S}_3 Z_6}{-\frac{B_{11} I_0 \omega_m^2}{A_{11}} + \hat{S}_3 Z_5 + J_1 \omega_m^2}$$

$$Z_{12} = -\frac{\mu_1 + \tilde{\mu}_2 (Z_1 + Z_5 Z_9)}{\mu_3}$$

$$Z_{13} = -\frac{\bar{\mu}_2 + \tilde{\mu}_2 (Z_2 + Z_5 Z_7)}{\mu_3}$$

$$Z_{14} = -\frac{\bar{\mu}_6 + \tilde{\mu}_2 (Z_3 + Z_5 Z_8)}{\mu_3}$$

$$Z_{15} = -\frac{\mu_2 + \tilde{\mu}_2 (Z_4 + Z_5 Z_{10})}{\mu_3}$$

$$Z_{16} = -\frac{\tilde{\mu}_2 (Z_6 + Z_5 Z_{11})}{\mu_3}$$

$$Z_{17} = -\frac{Z_8}{Z_7}$$

$$Z_{18} = -\frac{A_{11} Z_9 + B_{11} + I_0 \omega_m^2 Z_7}{A_{11} Z_7}$$

$$Z_{19} = -\frac{A_{11} Z_{10} - C_{11} + I_0 \omega_m^2 Z_8}{A_{11} Z_7}$$

$$Z_{20} = -\frac{A_{11}Z_{11} + I_0\omega_m^2 Z_{10} - \alpha I_3\omega_m^2}{A_{11}Z_7}$$

$$Z_{21} = -\frac{I_0\omega_m^2 Z_9 + J_1\omega_m^2}{A_{11}Z_7}$$

$$Z_{22} = -\frac{I_0\omega_m^2 Z_{11}}{A_{11}Z_7}$$

$$\bar{Z}_{17} = -\frac{B_{11}Z_8 + \hat{S}_3 Z_{14}}{B_{11}Z_7 + \hat{S}_3 Z_{13}}$$

$$\bar{Z}_{18} = -\frac{B_{11}Z_9 + \hat{S}_1 + \hat{S}_3 Z_{12} + J_1\omega_m^2 Z_7}{B_{11}Z_7 + \hat{S}_3 Z_{13}}$$

$$\bar{Z}_{19} = -\frac{B_{11}Z_{10} + \hat{S}_2 + \hat{S}_3 Z_{15} + J_1\omega_m^2 Z_8}{B_{11}Z_7 + \hat{S}_3 Z_{13}}$$

$$\bar{Z}_{20} = -\frac{B_{11}Z_{11} + X_{55} + \hat{S}_3 Z_{16} + J_1\omega_m^2 Z_{10} - \alpha J_4\omega_m^2}{B_{11}Z_7 + \hat{S}_3 Z_{13}}$$

$$\bar{Z}_{21} = -\frac{X_{55} + J_1\omega_m^2 Z_9 + (J_2 - \alpha J_4)\omega_m^2}{B_{11}Z_7 + \hat{S}_3 Z_{13}}$$

$$\bar{Z}_{22} = -\frac{J_1\omega_m^2 Z_{11}}{B_{11}Z_7 + \hat{S}_3 Z_{13}}$$

$$Z_{23} = \frac{\bar{Z}_{17} - Z_{17}}{Z_{18} - \bar{Z}_{18}}$$

$$Z_{24} = \frac{\bar{Z}_{19} - Z_{19}}{Z_{18} - \bar{Z}_{18}}$$

$$Z_{25} = \frac{\bar{Z}_{20} - Z_{20}}{Z_{18} - \bar{Z}_{18}}$$

$$Z_{26} = \frac{\bar{Z}_{21} - Z_{21}}{Z_{18} - \bar{Z}_{18}}$$

$$Z_{27} = \frac{\bar{Z}_{22} - Z_{22}}{Z_{18} - \bar{Z}_{18}}$$

$$\xi_1 = \xi_7$$

$$\xi_2 = \xi_8 - Z_{26}\xi_7 + \xi_8$$

$$\xi_3 = \xi_9 - Z_{23} - Z_{26}\xi_8$$

$$\xi_4 = \xi_{10} - Z_{24} + Z_{26}\xi_9$$

$$\xi_5 = \xi_{11} - Z_{25} + Z_{26}\xi_{10}$$

$$\xi_6 = -Z_{27} - Z_{26}\xi_{11}$$

$$\xi_7 = \frac{Z_{23}}{Z_{21} + Z_{18}Z_{26} - Z_{26}^2}$$

$$\begin{aligned}
\xi_8 &= \frac{Z_{24} + Z_{26}Z_{23} - Z_{17} - Z_{18}Z_{23}}{Z_{21} + Z_{18}Z_{26} - Z_{26}^2} \\
\xi_9 &= \frac{Z_{25} + Z_{26}Z_{24} - Z_{19} - Z_{18}Z_{24}}{Z_{21} + Z_{18}Z_{26} - Z_{26}^2} \\
\xi_{10} &= \frac{Z_{27} + Z_{26}Z_{25} - Z_{20} - Z_{18}Z_{25}}{Z_{21} + Z_{18}Z_{26} - Z_{26}^2} \\
\xi_{11} &= \frac{Z_{26}Z_{27} - Z_{18}Z_{27} - Z_{22}}{Z_{21} + Z_{18}Z_{26} - Z_{26}^2} \\
\bar{\xi}_1 &= A_{66}\bar{\xi}_4 + B_{66} \\
\bar{\xi}_2 &= I_0\omega_m^2\bar{\xi}_4 + A_{66}\bar{\xi}_5 \\
\bar{\xi}_3 &= I_0\omega_m^2\bar{\xi}_5 + J_1\omega_m^2 \\
\bar{\xi}_4 &= \frac{B_{66}^2 - A_{66}X_{66}}{B_{66}\omega_m^2(J_1 - I_1)} \\
\bar{\xi}_5 &= \frac{-X_{55} + (J_1 - J_2 + \alpha J_4)\omega_m^2}{J_1 - I_0}
\end{aligned} \tag{A.11}$$

$$T_1 = -2\beta e_{15}h^2h_p - 2\beta e_{15}hh_p^2 - \frac{2}{3}\beta e_{15}h_p^3 + 2e_{15}h_p \tag{A.12}$$

For open circuit condition

$$\begin{aligned}
\bar{T}_1 &= -\frac{16}{3}\bar{\Xi}_{11}h_p \\
\bar{T}_1 &= \frac{\bar{\Xi}_{11}\bar{e}_{31}h_p^2(ah^3 + 3ah^2h_p + 3\alpha hh_p^2 + ah_p^3 - h - h_p)}{\bar{\Xi}_{33}} \\
\bar{T}_2 &= \frac{\alpha\bar{\Xi}_{11}\bar{e}_{31}h_p^2(h + h_p)^3}{\bar{\Xi}_{33}}
\end{aligned} \tag{A.13}$$

And for closed circuit condition

$$\bar{T}_1 = -\frac{4}{3}\bar{\Xi}_{11}h_p, \quad \bar{T}_1 = 0, \quad \bar{T}_2 = 0 \tag{A.14}$$

References

- [1] Mindlin RD. Influence of rotator inertia and shear in flexural motion of isotropic, elastic plates. *J Appl Mech* 1951; 18: 31-38.
- [2] Reddy JN. A simple higher-order theory for laminated plates. *J Appl Mech* 1984; 51: 745-52.
- [3] Banhart J. Aluminum Foams: On the road to real applications. *Mrs Bulletin* 2003; 28(04): 290-295.
- [4] Leissa AW. The free vibration of rectangular plates. *J Sound Vibr* 1973; 31: 273–293.
- [5] Reddy JN, Phan ND. Stability and free vibration of isotropic, orthotropic and laminated plates according to higher-order shear deformation theories. *J Sound Vibr* 1985; 98: 157–170.
- [6] Liew KM, Hung KC, Lim MK. A continuum three-dimensional vibration analysis of thick rectangular plates. *Int J Solids Struct* 1993; 30: 3357-3379.
- [7] Vel SS, Batra RC. Three-dimensional exact solution for the vibration of functionally graded rectangular plates. *J Sound Vibr* 2004; 272: 703–30.
- [8] Ferreira AJM, Batra RC, Roque CMC, Qian LF, Jorge RMN. Natural frequencies of functionally graded plates by a meshless method. *Compos Struct* 2006; 75: 593–600.
- [9] Matsunaga H. Free vibration and stability of functionally graded plates according to a 2-D higher-order deformation theory. *Compos Struct* 2008; 82: 499-512.
- [10] Hasani Baferani A, Saidi AR, Ehteshami H. Accurate solution for free vibration analysis of functionally graded thick rectangular plates resting on elastic foundation. *Compos Struct* 2011. 93(7): 1842–53.
- [11] Jin G, Sou Z, Shi S, Ye T, Gao S. Three-dimensional exact solution for free vibration of arbitrary thick functionally graded plates with general boundary conditions. *Compos Struct* 2014; 108: 565-577.
- [12] Hwang WS, Park HC, Hwang WB. Vibration control of laminated plate with piezoelectric sensors and actuators: Finite element formulation and model analysis. *J Intell Mater Syst Struct* 1993; 4: 317-329.
- [13] Heyliger P, Saravanos DA. Exact free-vibration analysis of laminated plates with embedded piezoelectric layers. *J Acoust Soc Am* 1995; 98(3): 1547-1557.
- [14] Liang XQ, Batra RC. Changes in frequencies of a laminated plate caused by embedded piezoelectric layers. *AIAA J* 1997; 35: 1672-3.
- [15] He XQ, Ng TY. Active control of fGM plates with integrated piezoelectric sensors and actuators. *Int J Solids Struct* 2001; 38: 1641-1655.
- [16] Baillargeon BP, Vel SS. Exact solution for the vibration and active damping of composite plates with piezoelectric shear actuators. *J Sound Vibr* 2005; 282: 781-804.
- [17] Pietrzakowski M. Piezoelectric control of composite plate vibration: Effect of electric potential distribution. *Comp Struct* 2008; 86: 948-54.
- [18] Askari Farsangi MA, Saidi AR. Levy type solution for free vibration analysis of functionally graded rectangular plates with piezoelectric layers. *Smart Mater Struct* 2012; 21: 094017 (15pp).

- [19] Askari Farsangi MA, Saidi AR, Batra RC. Analytical solution for free vibrations of moderately thick hybrid piezoelectric laminated plates. *J Sound Vibr* 2013; 332: 5981-5998.
- [20] Theodorakopoulos DD, Beskos DE. Flexural vibration of poroelastic plates. *Acta Mech* 1994; 103:191-203.
- [21] Leclaire P, Horoshenkov KV, Cummings A. Transverse vibrations of a thin rectangular porous plate saturated by a fluid. *J Sound Vibr* 2001; 247: 1-18.
- [22] Magnucka-Blandzi E. Vibration of a porous-cellular circular plate. *Appl Math Mech* 2006; 6: 243-244.
- [23] Magnucka-Blandzi E. Axi-symmetrical deflection and buckling of circular porous-cellular plate. *Thin Wall Struct* 2008; 46: 333-37.
- [24] Khosrshidvand AR, Joubaneh EF, Jabbari M, Eslami MR. Buckling analysis of a porous circular plate with piezoelectric sensor-actuator layers under uniform radial compression. *Acta Mech* 2014; 225: 179-193.
- [25] Rezaei AS, Saidi AR. Exact solution for free vibration of thick rectangular plates made of porous materials. *Compos Struct* 2015; 134: 1051-1060.
- [26] Rezaei AS, Saidi AR. Application of Carrera Unified Formulation to study the effect of porosity on natural frequencies of thick porous-cellular plates. *Compos Part B: Eng* 2016; 91: 361-370.
- [27] Yong J. *Special topics in the theory of piezoelectricity*. Springer 2009; 11-16.
- [28] Wang Q, Quek ST, Sun CT, Liu X. Analysis of piezoelectric coupled circular plate. *Smart Mater Struct* 2001; 10: 229-239.
- [29] Wu N, Wang Q, Quek ST. Free vibration analysis of piezoelectric coupled circular plate with open circuit. *J Sound Vibr* 2010; 329: 1126-1136.
- [30] Jalili N. *Piezoelectric-based vibration control*. Springer 2010; 131-133.
- [31] Rahmat Talabi M, Saidi AR. An explicit exact analytical approach for free vibration of circular/annular functionally graded plates bonded to piezoelectric actuator/sensor layers based on Reddy's plate theory. *Appl Math Model* 2013; 37(14): 7664-7684.
- [32] Rouzegar J, Abad F. Free vibration analysis of FG plate with piezoelectric layers using four-variable refined plate theory. *Thin Wall Struct* 2015; 89: 76-83.
- [33] Malik M, Bert CW. Three-dimensional elasticity solutions for free vibrations of rectangular plates by the differential quadrature method. *Int J Solids Struct* 1998; 35: 299-318.
- [34] Hosseini-Hashemi Sh, Fadaee M, Atashipour SR. Study on the free vibration of thick functionally graded rectangular plates according to a new exact closed-form procedure. *Compos Struct* 2011; 93: 722-735.

Figure Captions:

Figure 1. The geometry and coordinate system for porous-cellular rectangular plate surrounded by two piezoelectric layers.

Figure 2. The variation of elastic modulus through the thickness of plate

Figure 3. The variation of natural frequency of a coupled porous plate under various boundary conditions with closed circuit piezoelectric layers versus aspect ratio ($2h/a=0.1$, $e_0=0.5$, $h_p/2h=0.1$).

Figure 4. The variation of NFD parameter versus the thickness ratio for a piezoelectric coupled porous plate under different boundary conditions ($2h/a=0.1$, $e_0=0.3$, $a/b=1$): (a) Closed circuit (b) Open circuit

Figure 5. The variation of NFD parameter versus the thickness ratio of a closed circuit piezoelectric coupled porous plate for different thickness-length ratios, ($e_0=0.3$, $a/b=1$): (a) SSSF, (b) SSSS

Figure 6. The variation of NFD parameter of a square plate under SFSF boundary condition versus the thickness ratio for different coefficients of plate porosity ($2h/a=0.15$): (a) Closed circuit (b) Open circuit

Figure 7. The variation of fundamental natural frequency of a porous square plate versus the coefficient of plate porosity for various boundary conditions ($a=b=1m$, $h_p=0$, $Mass=Constant=400Kg$, $h \neq Constant$).

Figure 8. The variation of fundamental natural frequency of piezoelectric coupled porous plate versus the coefficient of plate porosity for various boundary conditions ($a=b=1m$, $h_p=0.01m=Constant$, $Mass=400Kg=Constant$, $h \neq Constant$), a) Closed circuit and b) Open circuit

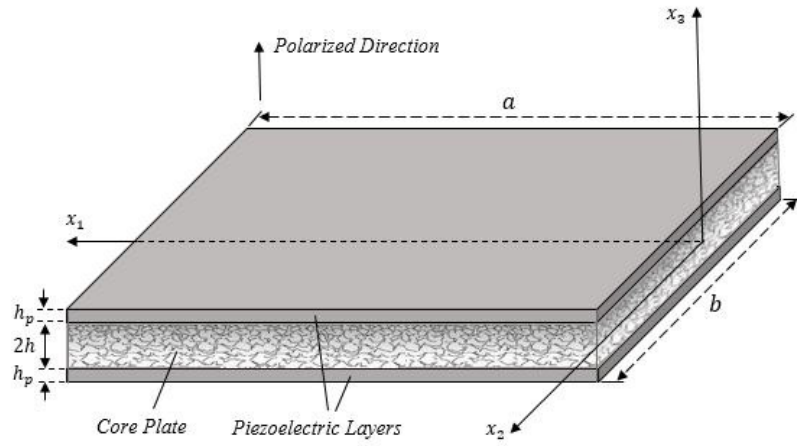


Figure 1. The geometry and coordinate system for porous-cellular rectangular plate surrounded by two piezoelectric layers

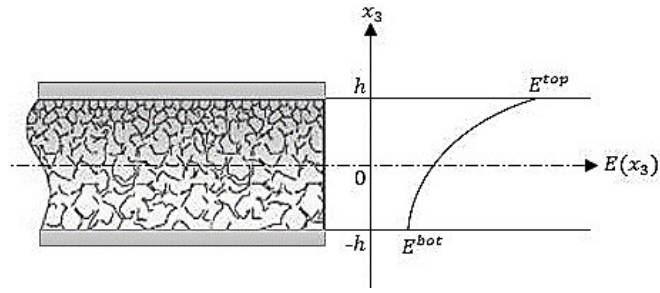


Figure 2. The variation of elastic modulus through the thickness of plate

ACCEPTED MANUSCRIPT

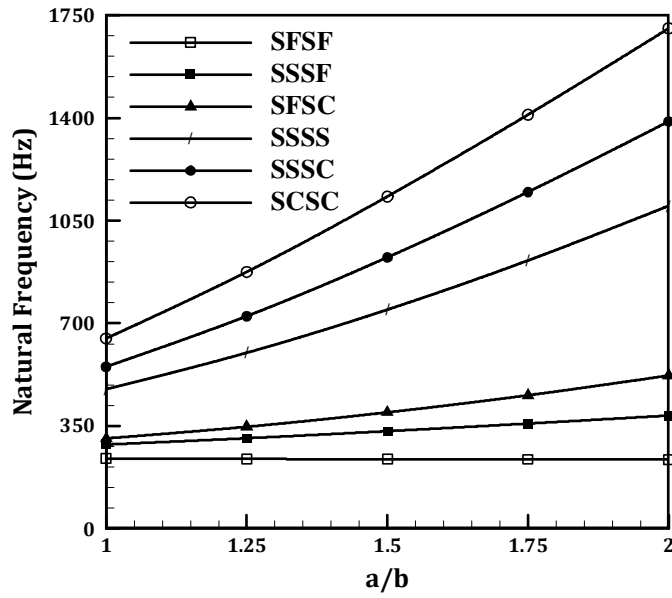


Figure 3. The variation of natural frequency of a coupled porous plate under various boundary conditions versus aspect ratio with closed circuit piezoelectric layers ($2h/a=0.1$, $e_0=0.5$, $h_p/2h=0.1$).

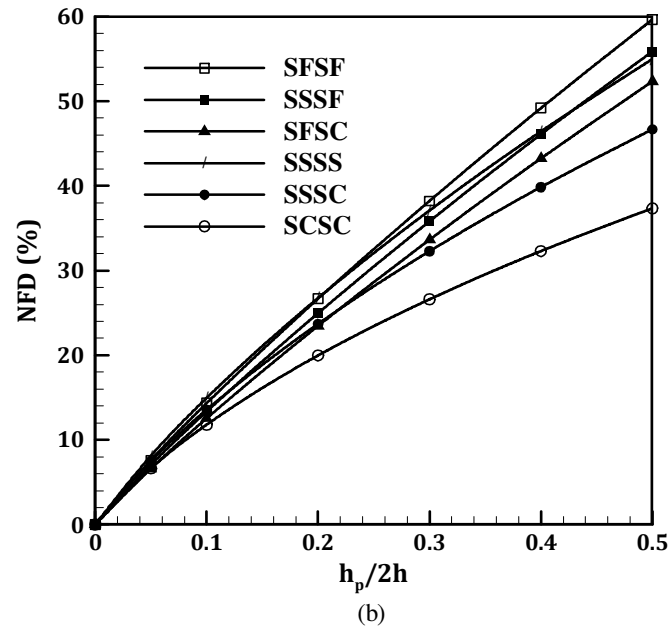
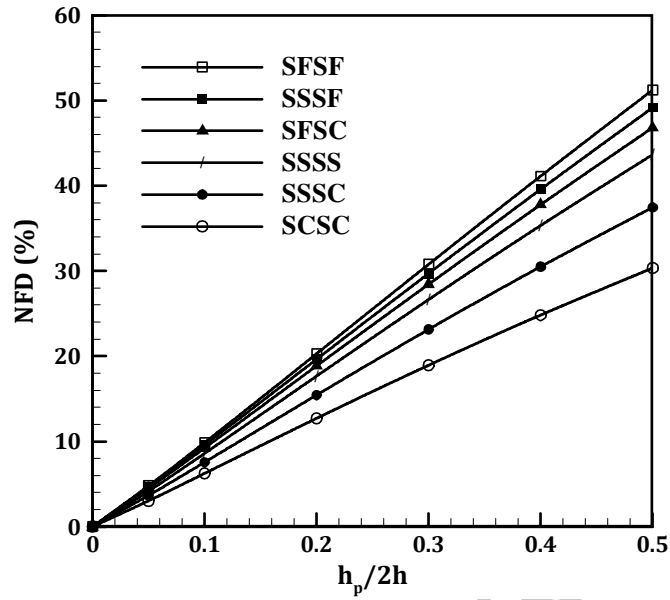


Figure 4. The variation of NFD parameter versus the thickness ratio for a piezoelectric coupled porous plate under different boundary conditions ($2h/a=0.1$, $e_0=0.3$, $a/b=1$): (a) Closed circuit (b) Open circuit

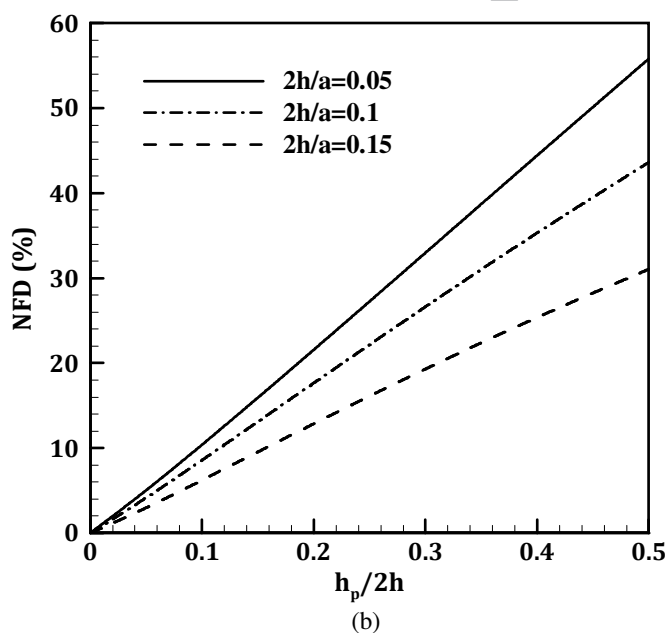
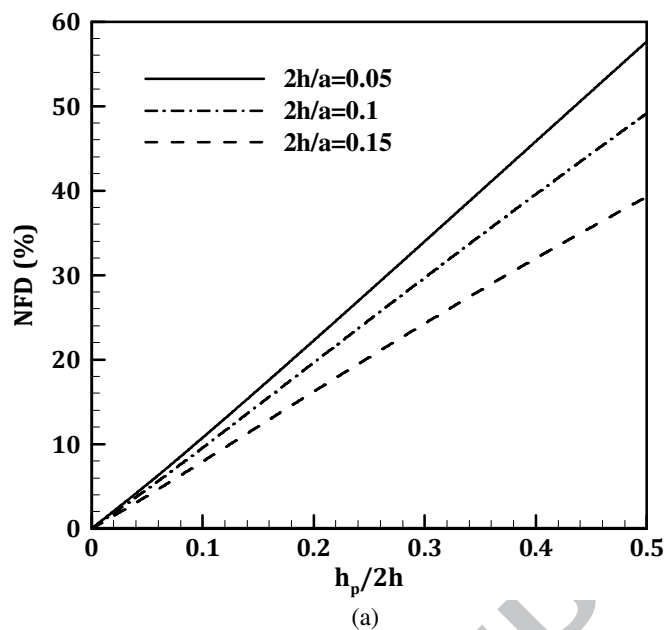


Figure 5. The variation of NFD parameter versus the thickness ratio of a closed circuit piezoelectric coupled porous plate for different thickness-length ratios, ($e_0=0.3$, $a/b=1$): (a) SSSF, (b) SSSS

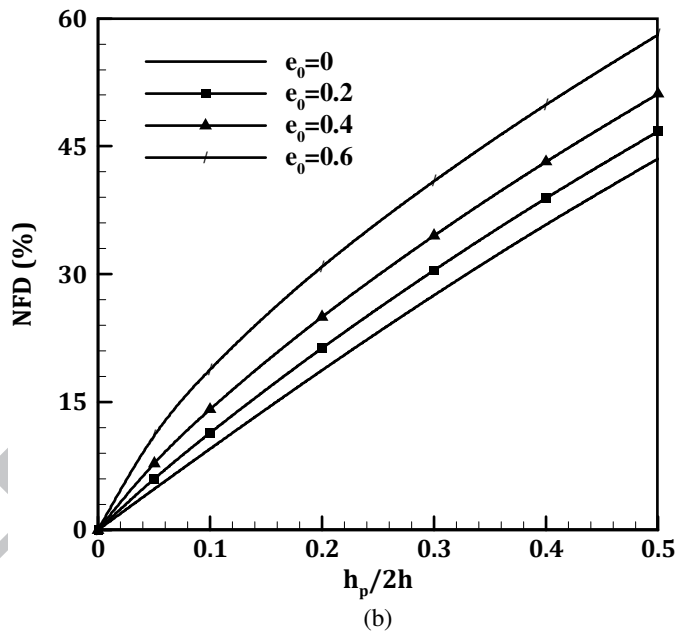
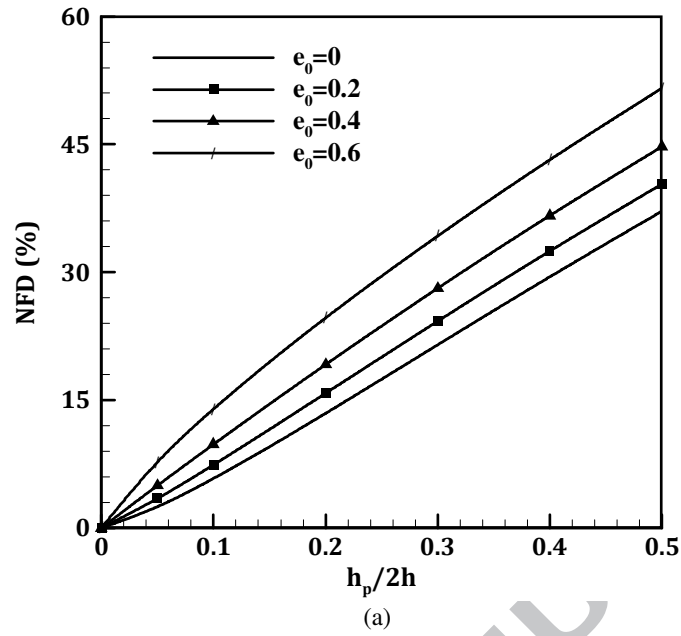


Figure 6. The variation of NFD parameter of a square plate under SFSF boundary condition versus the thickness ratio for different coefficients of plate porosity ($2h/a=0.15$): (a) Closed circuit (b) Open circuit

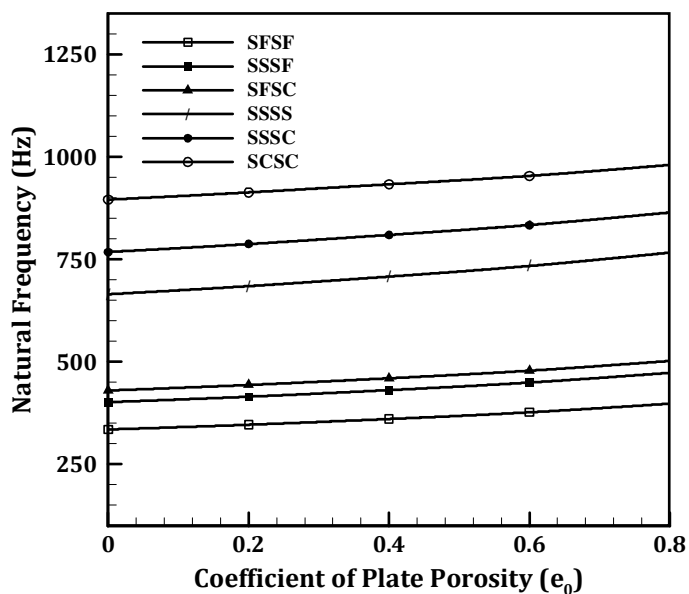
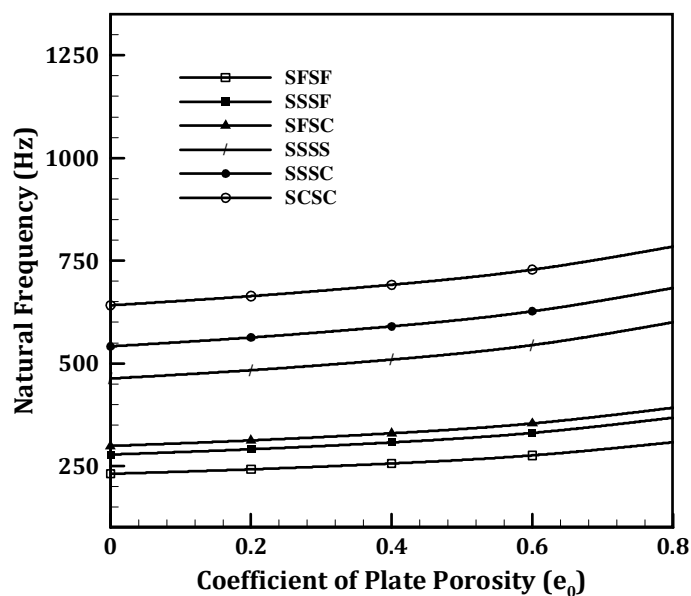
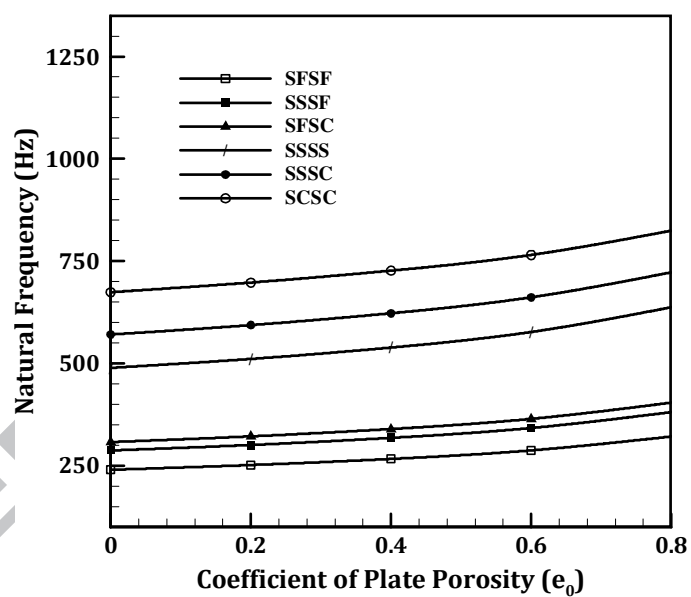


Figure 7. The variation of fundamental natural frequency of a porous square plate versus the coefficient of plate porosity for various boundary conditions ($a=b=1m$, $h_p=0$, $Mass=Constant=400Kg$, $h \neq Constant$).



(a)



(b)

Figure 8. The variation of fundamental natural frequency of piezoelectric coupled porous plate versus the coefficient of plate porosity for various boundary conditions ($a=b=1m$, $h_p=0.01m=Constant$, $Mass=400Kg=Constant$, $h \neq Constant$), a) Closed circuit and b) Open circuit

Table captions

- Table 1.** The properties of piezoelectric and porous materials
- Table 2.** Comparison of the non-dimensional fundamental natural frequency for a simply supported homogeneous and isotropic plate
- Table 3.** Comparison of the non-dimensional fundamental natural frequency for a homogeneous plate under various mechanical boundary conditions
- Table 4.** Comparison of the first ten natural frequencies (Hz) for a simply supported piezoelectric coupled homogeneous and isotropic plate
- Table 5.** The first three natural frequencies (Hz) of SFSF and SSSS piezoelectric coupled porous plate ($h_p/2h=0.05$, $a/b=1$).
- Table 6.** The first three natural frequencies (Hz) of SCSC and SSSF piezoelectric coupled porous plate ($h_p/2h=0.05$, $a/b=1$)
- Table 7.** The first three natural frequencies (Hz) of SFSC and SSSC piezoelectric coupled porous plate ($h_p/2h=0.05$, $a/b=1$)
- Table 8.** Effect of the electrical condition on the fundamental natural frequency of the piezoelectric coupled plate under Levy-type boundary conditions for different thickness ratios ($2h/a=0.15$, $e_0=0.2$, $a/b=1$).
- Table 9.** Effect of electrical condition on the first three natural frequencies of the piezoelectric coupled plate under Levy-type boundary conditions ($2h/a=0.15$, $h_p/2h=0.1$, $e_0=0.2$, $a/b=1$).

Table 1. The properties of piezoelectric and porous materials

Material	Piezoelectric layers				Core Plate	
	PZT-4	PZT-8	PZT-6B	PIC-151	Cellular Aluminum	
Elastic constants (GPa)	c_{11}	132	137	168	107.6	---
	c_{12}	71	69.9	84.7	63.1	
	c_{13}	73	71.1	84.2	63.9	
	c_{33}	115	123	163	100.4	
	c_{55}	26	31.3	35.5	19.6	
Piezoelectric coefficients (C/m ²)	e_{33}	14.1	17.5	7.1	15.14	---
	e_{31}	-4.1	-4.0	-0.9	-9.52	
	e_{15}	10.5	10.4	4.6	11.97	
Dielectric constants (nC/Vm)	ϵ_{11}	7.124	7.97	3.60	9.837	---
	ϵ_{22}	6.46	7.97	3.60	9.837	
	ϵ_{33}	5.841	5.14	3.42	8.190	
Density (Kg/m ³)	ρ	7500	7600	7550	7800	2707
Young modulus (GPa)	E	---	---	---	---	70

Table 2. Comparison of the non-dimensional fundamental natural frequency for a simply supported homogeneous and isotropic plate

Method		Present	2D HDT [9]	3D Method [11]	3D Elasticity [33]	Exact TSDT [34]
2h/a	0.1	0.0577	0.0577	0.0578	0.0577	0.577
	$1/\sqrt{10}$	0.4622	0.4658	0.4658	0.4658	0.4623

ACCEPTED MANUSCRIPT

Table 3. Comparison of the non-dimensional fundamental natural frequency for a homogeneous plate under various mechanical boundary conditions

BC's	2h/a	Present	TSDT [10]	3D Elasticity [11]
SSSS	0.1	0.1134	0.1134	0.1135
	0.2	0.4154	0.4154	0.4169
SFSF	0.1	0.0562	0.0562	0.0562
	0.2	0.2140	0.2141	0.2141
SCS C	0.1	0.1589	0.1589	0.1604
	0.2	0.5364	0.5363	0.5402
SSSF	0.1	0.0677	0.0678	0.0677
	0.2	0.2550	0.2552	0.2550
SSSC	0.1	0.1333	0.1333	0.1339
	0.2	0.4706	0.4706	0.4731
SFSC	0.1	0.0729	0.0730	0.0731
	0.2	0.2712	0.2714	0.2713

Table 4. Comparison of the first ten natural frequencies (Hz) for a simply supported piezoelectric coupled homogeneous and isotropic plate

Method	Mode Sequence									
	1	2	3	4	5	6	7	8	9	10
Present	144.49	360.90	360.90	576.92	720.72	720.72	936.10	936.10	1222.68	1222.68
CPT [15]	144.25	359.00	359.00	564.10	717.80	717.80	908.25	908.25	1223.14	1223.14
Diff. (%)	0.17	0.53	0.53	2.27	0.41	0.41	3.07	3.07	-0.04	-0.04
FSDT [18]	145.35	363.05	363.05	580.35	725.00	725.00	941.64	941.64	1229.88	1229.88
Diff. (%)	-0.59	-0.59	-0.59	-0.59	-0.59	-0.59	-0.59	-0.59	-0.58	-0.58
Navier [32]	145.35	363.06	363.06	580.37	725.03	725.03	941.69	941.69	1229.96	1229.96
Diff. (%)	-0.59	-0.59	-0.59	-0.59	-0.59	-0.59	-0.59	-0.59	-0.59	-0.59

ACCEPTED MANUSCRIPT

Table 5. The first three natural frequencies (Hz) of SFSF and SSSS piezoelectric coupled porous plate ($h_p/2h=0.05$, $a/b=1$).

2h/a	EC's	Coefficient of Plate Porosity (ϵ_0)								
		0			0.25			0.5		
		Mode Sequence			Mode Sequence			Mode Sequence		
		1 st	2 nd	3 rd	1 st	2 nd	3 rd	1 st	2 nd	3 rd
SFSF										
0.05	Closed	121.301 (1,1)	200.764 (1,2)	450.892 (1,3)	118.401 (1,1)	195.912 (1,2)	439.752 (1,3)	114.893 (1,1)	190.058 (1,2)	426.309 (1,3)
	Open	124.253 (1,1)	202.954 (1,2)	460.998 (1,3)	121.624 (1,1)	198.296 (1,2)	450.819 (1,3)	118.515 (1,1)	192.726 (1,2)	438.807 (1,3)
0.1	Closed	238.329 (1,1)	387.514 (1,2)	846.216 (1,3)	232.453 (1,1)	377.667 (1,2)	823.529 (1,3)	225.363 (1,1)	365.829 (1,2)	796.287 (1,3)
	Open	243.905 (1,1)	391.360 (1,2)	864.570 (1,3)	238.523 (1,1)	381.831 (1,2)	843.530 (1,3)	232.160 (1,1)	370.457 (1,2)	818.738 (1,3)
0.2	Closed	448.362 (1,1)	699.457 (1,2)	1114.689 (1,3)	436.250 (1,1)	679.434 (1,2)	1068.185 (1,3)	421.752 (1,1)	655.560 (1,2)	1019.189 (1,3)
	Open	457.879 (1,1)	705.147 (1,2)	1118.463 (1,3)	446.529 (1,1)	685.515 (1,2)	1072.392 (1,3)	433.149 (1,1)	662.198 (1,2)	1024.017 (1,3)
SSSS										
0.05	Closed	247.352 (1,1)	608.107 (1,2)	957.500 (2,2)	241.363 (1,1)	592.940 (1,2)	932.980 (2,2)	234.118 (1,1)	574.636 (1,2)	903.457 (2,2)
	Open	255.830 (1,1)	628.557 (1,2)	989.132 (2,2)	250.651 (1,1)	615.295 (1,2)	967.492 (2,2)	244.611 (1,1)	599.825 (1,2)	942.248 (2,2)
0.1	Closed	478.750 (1,1)	1129.345 (1,2)	1718.002 (2,2)	466.490 (1,1)	1097.946 (1,2)	1667.376 (2,2)	451.728 (1,1)	1060.441 (1,2)	1607.288 (2,2)
	Open	494.566 (1,1)	1164.453 (1,2)	1768.859 (2,2)	483.746 (1,1)	1136.003 (1,2)	1722.233 (2,2)	471.124 (1,1)	1102.874 (1,2)	1668.077 (2,2)
0.2	Closed	859.001 (1,1)	1838.226 (1,2)	2626.428 (2,2)	833.688 (1,1)	1776.570 (1,2)	2532.508 (2,2)	803.644 (1,1)	1704.623 (1,2)	2424.035 (2,2)
	Open	884.430 (1,1)	1885.951 (1,2)	2689.413 (2,2)	861.117 (1,1)	1827.400 (1,2)	2599.074 (2,2)	834.039 (1,1)	1760.047 (1,2)	2495.876 (2,2)

Table 6. The first three natural frequencies (Hz) of SCSC and SSSF piezoelectric coupled porous plate ($h_p/2h=0.05$, $a/b=1$)

2h/a	EC's	Coefficient of Plate Porosity (ϵ_0)								
		0			0.25			0.5		
		Mode Sequence			Mode Sequence			Mode Sequence		
	1 st	2 nd	3 rd	1 st	2 nd	3 rd	1 st	2 nd	3 rd	
SCSC										
0.05	Closed	357.007 (1,1)	667.786 (2,1)	831.096 (1,2)	348.087 (1,1)	650.829 (2,1)	809.319 (1,2)	337.336 (1,1)	630.413 (2,1)	783.202 (1,2)
	Open	368.950 (1,1)	689.916 (2,1)	857.940 (1,2)	361.136 (1,1)	674.985 (2,1)	838.539 (1,2)	352.031 (1,1)	657.579 (2,1)	815.948 (1,2)
0.1	Closed	664.835 (1,1)	1216.125 (2,1)	1457.899 (1,2)	646.294 (1,1)	1181.102 (2,1)	1412.935 (1,2)	624.228 (1,1)	1139.494 (2,1)	1360.047 (1,2)
	Open	685.155 (1,1)	1252.540 (2,1)	1498.401 (1,2)	668.293 (1,1)	1220.448 (2,1)	1456.380 (1,2)	648.710 (1,1)	1183.181 (2,1)	1407.832 (1,2)
0.2	Closed	1091.656 (1,1)	1920.632 (2,1)	2151.282 (1,2)	1055.057 (1,1)	1854.249 (2,1)	2071.313 (1,2)	1012.538 (1,1)	1777.246 (2,1)	1979.909 (1,2)
	Open	1118.851 (1,1)	1967.904 (2,1)	2197.960 (1,2)	1083.979 (1,1)	1904.420 (2,1)	2120.373 (1,2)	1043.987 (1,1)	1831.681 (2,1)	2032.407 (1,2)
SSSF										
0.05	Closed	146.731 (1,1)	344.061 (1,2)	509.019 (2,1)	143.213 (1,1)	335.642 (1,2)	496.427 (2,1)	138.960 (1,1)	325.475 (1,2)	481.231 (2,1)
	Open	149.816 (1,1)	352.917 (1,2)	522.549 (2,1)	146.579 (1,1)	345.340 (1,2)	511.175 (2,1)	142.740 (1,1)	336.426 (1,2)	497.777 (2,1)
0.1	Closed	286.863 (1,1)	655.114 (1,2)	954.158 (1,2)	279.724 (1,1)	637.900 (1,2)	928.172 (2,1)	271.119 (1,1)	617.220 (1,2)	897.085 (2,1)
	Open	292.582 (1,1)	671.298 (1,2)	977.255 (2,1)	285.942 (1,1)	655.537 (1,2)	953.14 (2,1)	278.072 (1,1)	637.017 (1,2)	924.819 (2,1)
0.2	Closed	532.727 (1,1)	1135.377 (1,2)	1286.463 (1,3)	518.031 (1,1)	1100.665 (1,2)	1232.829 (1,3)	500.480 (1,1)	1059.343 (1,2)	1176.410 (1,3)
	Open	542.094 (1,1)	1160.534 (1,2)	1289.232 (1,3)	528.123 (1,1)	1127.751 (1,2)	1235.919 (1,3)	511.631 (1,1)	1089.239 (1,2)	1179.999 (1,3)

Table 7. The first three natural frequencies (Hz) of SFSC and SSSC piezoelectric coupled porous plate ($h_p/2h=0.05$, $a/b=1$)

2h/a	EC's	Coefficient of Plate Porosity (e_0)								
		0			0.25			0.5		
		Mode Sequence			Mode Sequence			Mode Sequence		
		1 st	2 nd	3 rd	1 st	2 nd	3 rd	1 st	2 nd	3 rd
SFSC										
0.05	Closed	158.837 (1,1)	406.442 (1,2)	514.619 (2,1)	155.012 (1,1)	396.337 (1,2)	501.866 (2,1)	150.390 (1,1)	384.154 (1,2)	486.480 (2,1)
	Open	161.829 (1,1)	417.200 (1,2)	527.910 (2,1)	158.274 (1,1)	408.102 (1,2)	516.349 (2,1)	154.051 (1,1)	397.417 (1,2)	502.722 (2,1)
0.1	Closed	308.659 (1,1)	758.935 (1,2)	962.623 (2,1)	300.874 (1,1)	738.138 (1,2)	936.311 (2,1)	291.510 (1,1)	713.286 (1,2)	904.852 (2,1)
	Open	314.121 (1,1)	777.658 (1,2)	985.234 (2,1)	306.805 (1,1)	758.458 (1,2)	960.750 (2,1)	298.129 (1,1)	735.972 (1,2)	931.977 (2,1)
0.2	Closed	564.881 (1,1)	1258.425 (1,2)	1596.724 (2,1)	548.911 (1,1)	1217.483 (1,2)	1544.622 (2,1)	529.908 (1,1)	1169.252 (1,2)	1483.589 (2,1)
	Open	573.603 (1,1)	1284.792 (1,2)	1627.628 (2,1)	558.285 (1,1)	1245.656 (1,2)	1577.483 (2,1)	540.231 (1,1)	1200.077 (1,2)	1519.276 (2,1)
SSSC										
0.05	Closed	294.344 (1,1)	634.172 (2,1)	713.547 (1,2)	287.122 (1,1)	618.238 (2,1)	695.329 (1,2)	278.399 (1,1)	599.028 (2,1)	673.407 (1,2)
	Open	304.332 (1,1)	655.372 (2,1)	737.100 (1,2)	298.052 (1,1)	641.400 (2,1)	721.025 (1,2)	290.731 (1,1)	625.105 (2,1)	702.288 (1,2)
0.1	Closed	560.379 (1,1)	1168.193 (2,1)	1289.312 (1,2)	545.473 (1,1)	1135.222 (2,1)	1251.536 (1,2)	527.617 (1,1)	1095.928 (2,1)	1206.759 (1,2)
	Open	578.293 (1,1)	1203.946 (2,1)	1327.299 (1,2)	564.953 (1,1)	1173.925 (2,1)	1292.504 (1,2)	549.419 (1,1)	1139.005 (2,1)	1252.139 (1,2)
0.2	Closed	965.731 (1,1)	1876.557 (2,1)	1996.510 (1,2)	935.425 (1,1)	1812.751 (2,1)	1925.731 (1,2)	899.821 (1,1)	1738.495 (2,1)	1844.019 (1,2)
	Open	992.201 (1,1)	1924.141 (2,1)	2043.868 (1,2)	963.793 (1,1)	1863.349 (2,1)	1975.833 (1,2)	930.992 (1,1)	1793.542 (2,1)	1898.138 (1,2)

Table 8. Effect of the electrical condition on the fundamental natural frequency of the piezoelectric coupled plate under Levy-type boundary conditions for different thickness ratios ($2h/a=0.15$, $e_0=0.2$, $a/b=1$).

BC's	$h_p/2h$	disregarding piezo-effect	considering piezo-effect			
			Closed	Diff. (%)	Open	Diff. (%)
SFSF	0.05	340.934	340.942	0.00002	349.220	2.42798
	0.1	353.894	353.942	0.01356	367.041	3.71495
	0.2	381.346	381.604	0.06766	399.811	4.84206
SSSS	0.05	668.983	669.005	0.00329	691.867	3.42071
	0.1	687.932	688.075	0.02079	724.321	5.28962
	0.2	728.572	729.352	0.10706	778.910	6.90913
SCSC	0.05	884.958	885.003	0.00508	911.326	2.97958
	0.1	896.483	896.766	0.03157	936.036	4.41202
	0.2	923.630	925.177	0.16749	972.901	5.33450
SSSF	0.05	407.693	407.701	0.00196	416.007	2.03928
	0.1	422.240	422.291	0.01208	435.301	3.09326
	0.2	453.019	453.290	0.05982	471.001	3.96937
SFSC	0.05	435.285	435.294	0.00207	443.100	1.79538
	0.1	449.708	449.764	0.01245	461.854	2.70086
	0.2	480.215	480.517	0.06289	496.618	3.41576
SSSC	0.05	766.251	766.282	0.00404	790.933	3.22114
	0.1	782.528	782.726	0.02530	820.775	4.88762
	0.2	818.143	819.234	0.13335	868.619	6.16958

Table 9. Effect of electrical condition on the first three natural frequencies of the piezoelectric coupled plate under Levy-type boundary conditions ($2h/a=0.15$, $h_p/2h=0.1$, $e_0=0.2$, $a/b=1$).

BC's	Mode Sequence	disregarding piezo-effect	considering piezo-effect			
			Closed	Diff. (%)	Open	Diff. (%)
SF _{SF}	1 st (1,1)	353.894	353.942	0.01356	367.041	3.71495
	2 nd (1,2)	559.283	559.321	0.00679	567.318	1.43666
	3 rd (1,3)	1026.257	1026.257	0.00000	1033.085	0.66533
SS _{SS}	1 st (1,1)	687.932	688.075	0.02079	724.321	5.28962
	2 nd (1,2)	1513.073	1513.469	0.02617	1582.809	4.60890
	3 rd (2,2)	2196.219	2196.892	0.03064	2288.325	4.19384
SC _{SC}	1 st (1,1)	896.483	896.766	0.03157	936.036	4.41209
	2 nd (2,1)	1592.042	1592.539	0.03122	1660.750	4.31572
	3 rd (1,2)	1814.216	1815.034	0.04509	1881.380	3.70210
SS _{SF}	1 st (1,1)	422.240	422.291	0.01208	435.301	3.09326
	2 nd (1,2)	918.344	918.502	0.01720	954.491	3.93611
	3 rd (1,3)	1184.504	1184.504	0.00000	1189.491	0.42102
SF _{SC}	1 st (1,1)	449.708	449.764	0.01245	461.854	2.70086
	2 nd (1,2)	1030.542	1030.783	0.02339	1068.722	3.70485
	3 rd (2,1)	1307.735	1307.996	0.01996	1351.948	3.38088
SS _{SC}	1 st (1,1)	782.528	782.726	0.02530	820.775	4.88762
	2 nd (2,1)	1549.478	1549.911	0.02794	1618.866	4.47815
	3 rd (1,2)	1664.163	1664.750	0.03527	1733.059	4.13998